

# A Partial Neandertal Foot From the Late Middle Paleolithic of Amud Cave, Israel

OSBJORN M. PEARSON

Department of Anthropology, MSC 01-1040, University of New Mexico, Albuquerque, NM 87131, USA; [ompear@unm.edu](mailto:ompear@unm.edu);

 <https://orcid.org/0000-0002-1814-7663>

ADRIÁN PABLOS

Centro Nacional de Investigación sobre la Evolución Humana (CENIEH), Paseo Sierra de Atapuerca 3, 09002 Burgos; and, Centro Mixto UCM-ISCIII de Investigación sobre Evolución y Comportamiento Humanos, c/Monforte de Lemos, 5, 28029 Madrid, SPAIN; [adrizaino@yahoo.es](mailto:adrizaino@yahoo.es);

 <https://orcid.org/0000-0003-1630-4941>

YOEL RAK

Department of Anatomy and Anthropology, Sackler School of Medicine, Tel Aviv University, Tel Aviv 69978, ISRAEL; [yoelrak@tauex.tau.ac.il](mailto:yoelrak@tauex.tau.ac.il)

ERELLA HOVERS

Institute of Archaeology, The Hebrew University of Jerusalem, Jerusalem 91905, ISRAEL; and, Institute of Human Origins, Arizona State University, P.O. Box 874101, Tempe, AZ 85287-4101, USA; [hovers@mail.huji.ac.il](mailto:hovers@mail.huji.ac.il);  <https://orcid.org/0000-0002-7855-6573>

submitted: 26 July 2019; revised: 17 May 2020; accepted 4 June 2020

## ABSTRACT

Excavations of Amud Cave in 1991–1994 yielded 14 hominin skeletal specimens (Amud 5–19) in addition to those recovered in the 1960s. Amud 9 is a partial right distal leg and foot that preserves portions of the distal tibia, talus, first metatarsal, first proximal phalanx, and a middle and distal phalanx of digit II–IV. The bones are fairly small and likely belonged to a female. The talus features a strongly projecting fibular articular facet in common with Neandertals and many tali from Sima de los Huesos. Discriminant analysis of the talus shows that its nearest match lies among tali from Sima de los Huesos, a result primarily attributable to its moderately enlarged posterior trochlear articular breadth. The first metatarsal falls among Neandertals in discriminant space. The pedal phalanges are short and broad, in common with other Neandertals. The length of the first metatarsal and talus predict a female's stature of 160–166 cm and the width of the talar trochlea predicts a body mass of 59.9 kg. The bones were found within anthropogenic deposits dated date to 55 ka, very close in time to the proposed main pulse of Neandertal interbreeding, as inferred from living people's DNA, and slightly before the first appearance of Upper Paleolithic industries.

## INTRODUCTION

The Middle to Upper Paleolithic transition in Israel and adjacent areas is a matter of extreme interest due to its arguable association with the dispersal of modern humans from Africa (Alex et al. 2017; Bar-Yosef 2000; Douka et al. 2013; Foley and Lahr 1997; Hublin 2015; Mellars 2005, 2006; Rak 1993; Rebollo et al. 2011; Rose and Marks 2014; Shea 2007, 2008). Many other scientists remain skeptical or agnostic about the role of a late dispersal of modern humans from Africa in transforming the material culture of Eurasia (e.g., Greenbaum et al. 2019a, 2019b; Kuhn and Zwyns 2014). Genetic evidence places the dispersal of modern humans from Africa at ~70–50 ka (DiGiorgio et al. 2009; Fagundes et al. 2007; Fu et al. 2013, 2014; Henn et al. 2012; Li and Durbin 2011; Mallick et al. 2016; Schiffels and Durbin 2014; Scozzari et al. 2012; Soares et al. 2012; Wei et al. 2012), close to the inferred date of interbreeding that has left a

~1–3% Neandertal contribution in the genome of living humans outside of Africa (Kuhlwilm et al. 2016; Meyer et al. 2012; Sankararaman et al. 2014, 2016; Prüfer et al. 2017). The major pulse of admixture from Neandertals dates to 1843–2018 generations ago (48,178–64,036 years ago) based on the 95% credible intervals of the average of DECODE and linkage disequilibrium (LD) data sets for Europeans (Sankararaman et al. 2012). Based on ancient DNA, the admixture predated the Ust'-Ishim individual, directly radiocarbon dated 45 ka, by 232–430 generations (6,728–12,470 years at 29 years per generation), i.e., 51.7–57.4 ka (Fu et al. 2014). The midpoint of these estimates for admixture falls at 55 ka, which is also the suggested uranium-series age for Manot 1, the earliest modern human from the Levant (Hershkovitz et al. 2015) and very close to the means for TL and ESR-TIMS ages for subunits B1 and B2 at Amud Cave (Rink et al. 2001; Valladas et al. 1999), the strata that

contained all but one of the hominin remains (Hovers et al. 1995; and see below).

Renewed excavation of Amud Cave (Figure 1) in 1991–1994 (Hovers 1998, 2004; Hovers et al. 1991, 1995), yielded 14 Neandertal specimens (Amud 5-19; Hovers et al. 1995; Rak et al. 1994), which add to the four specimens (Amud I-IV) recovered during excavations in the 1960s (Suzuki and Takai 1970). The original description of Amud I, an adult male skeleton recovered in 1961, emphasized the “progressive” morphology of the cranium (Suzuki, 1970) and aspects of the postcranial skeleton (Endo and Kimura 1970), which fit the dominant interpretation at the time that modern humans, as represented by the fossils from Skhul and Qafzeh, postdated and had evolved from “progressive” Neandertals in the Near East (Howell 1957, 1958; see discussion in Rak 1998). The hypothesis of an evolutionary sequence leading from Near Eastern Neandertals to the earliest modern humans remained influential (Smith et al. 1989; Trinkaus 1983, 1984), even in the face of faunal evidence that the early modern humans from Qafzeh predated most of the Levantine Neandertals (Bar-Yosef and Vandermeersch 1981), a deduction that was substantiated by subsequent TL and ESR dates for Qafzeh (Schwarcz et al. 1988; Valladas et al. 1987, 1988, 1998) and Skhul (Mercier et al. 1993; Stringer et al. 1989).

During the 1990s, emphasis shifted from general comparisons of proportions and morphological details (McCown and Keith 1939; Trinkaus 1983, 1984; Vandermeersch 1981) to cladistic features that differentiated Neandertal and modern human crania and postcrania (e.g., Rak 1986, 1990, 1991; Rak and Arensburg 1987; Rak et al. 1994, 1996; Tillier 1989). Within this perspective, at least three hominins from Amud (Amud I, II, and 7) possessed derived features of Neandertals and thus could be considered as such (Hovers et al. 1995; Lavi 1994). At the same time, other authors noted that in some features Neandertals and early modern humans from Skhul and Qafzeh overlapped (Arensburg 1991; Arensburg and Belfer-Cohen 1998; Trinkaus 1995), sometimes in ways that separated both from more recent humans (Rhodes and Trinkaus 1977; Tillier 1989, 1998, 1999; Vandermeersch 1981).

The temporal context of Amud Cave, the presence of hominin fossils, and the rich archaeological record excavated from the site (see below) have rendered it a key site for questions related to the shift from the Middle to the Upper Paleolithic in the Levant. The current paper describes and analyzes the Amud 9 fossil and presents some implications of how it might inform the discussion.

## OVERVIEW OF THE SITE OF AMUD

The Middle Paleolithic (MP) occupation of Amud Cave is known through a series of publications pertaining to its chronology, site formation processes, human remains, lithic typology, raw material acquisition and use, climatic shifts based on faunal and isotopic studies, plant use, hunting territories, and spatial organization of the cave's use (Alperson-Afil and Hovers 2005; Belmaker and Hovers 2011; Ekshtain et al. 2017; Hallin et al. 2012; Hartman et al.

2015; Hovers 2004, 2007; Hovers et al. 1995, 2000, 2011; Kol-ska Horwitz and Hongo 2008; Krakovsky 2017; Madella et al. 2002; Rabinovich and Hovers 2004; Rak et al. 1994; Rink et al. 2001; Shahack-Gross et al. 2008; Suzuki and Takai 1970; Valladas et al. 1999; Zeigen et al. 2019). Spatial studies of Middle Paleolithic remains often focus on sites with relatively low densities of finds and with clear stratigraphic and spatial features that help distinguish demarcated areas within sites. Sites with complex stratigraphies, high find densities and no clear spatial features are less often studied. Here we re-report on a case study from the Neandertal site of Amud Cave (Israel). The site's stratigraphy, initially established in the 1960s (Chinzei 1970), was confirmed and elaborated by the later excavations (Hovers 2004; Hovers et al. 1991, 2017). Apart from disturbed sediments of Unit A, which contained historic artifacts or a mix of prehistoric lithics and historical artifacts, all the sediments at the site are MP in age (Unit B). Stratigraphic subunit B4 directly overlies bedrock and has a weighted mean Thermoluminescence (TL) date of  $68.5 \pm 3.4$  ka (Valladas et al. 1999). Subunit B3 is archaeologically sterile and consists of gravel from the disintegration of the cave roof and walls. The overlying subunits B2 and B1 produced weighted average ages of  $56.5 \pm 3.5$  ka, and  $57.6 \pm 3.7$  ka, respectively (Valladas et al. 1999). Notably, the ages of subunits B2 and B1 are statistically indistinguishable, indicating a period of rapid deposition from more intensive or frequent occupation of the site (Hovers 2004; Hovers et al. 2017). Combined electron spin resonance (ESR) and thermal ionization mass spectrometric (TIMS)  $^{230}\text{Th}/^{234}\text{U}$  analysis of six teeth provided ages of  $53 \pm 8$  ka for subunit B1,  $61 \pm 9$  ka for B2, and  $70 \pm 11$  ka (Rink et al. 2000; a single date of  $113 \pm 18$  ka subunit B4 is considered an unexplained outlier). Thus, the absolute dates largely agree and indicate that almost all the MP hominins from the site derive from subunits B2 and B1 (Hovers et al. 1995; see Figure 1). The sole exception is Amud IV, a temporal bone of a three-year-old child, described by Suzuki and Takai as originating from subunit B4. The dates place the Amud hominins among the last Neandertals known from the Levant. The cave's roof started collapsing during the time of deposition of subunit B3 and continued during the deposition of B2. Much of the large debris from this collapse appears to have washed into the drainage when the Late Pleistocene Rift Valley lakes started drying out and the erosional base deepened (Inbar and Hovers 1999).

Watanabe's (1970) analysis of the lithics from the site concluded that they belonged to a transitional industry between the MP and Upper Paleolithic (UP). Ohnuma's (1992) small-scale study later analyses (of a larger sample of lithics: Alperson-Afil and Hovers 2005; Hovers 1998, 2004, 2007) concluded that the Amud assemblages fell within the range of variability of later MP (100–55 ka) assemblages from the Levant, with an extensive use of unipolar Levallois flaking combined with the use of centripetal modes. In sites such as Tabun, Dederiyeh, and Kebara, broadly similar assemblages are associated with Neandertals, but variability is high among assemblages and this relationship is not exclusive (e.g., Abadi et al. 2020; Ekshtain and Tryon 2019;

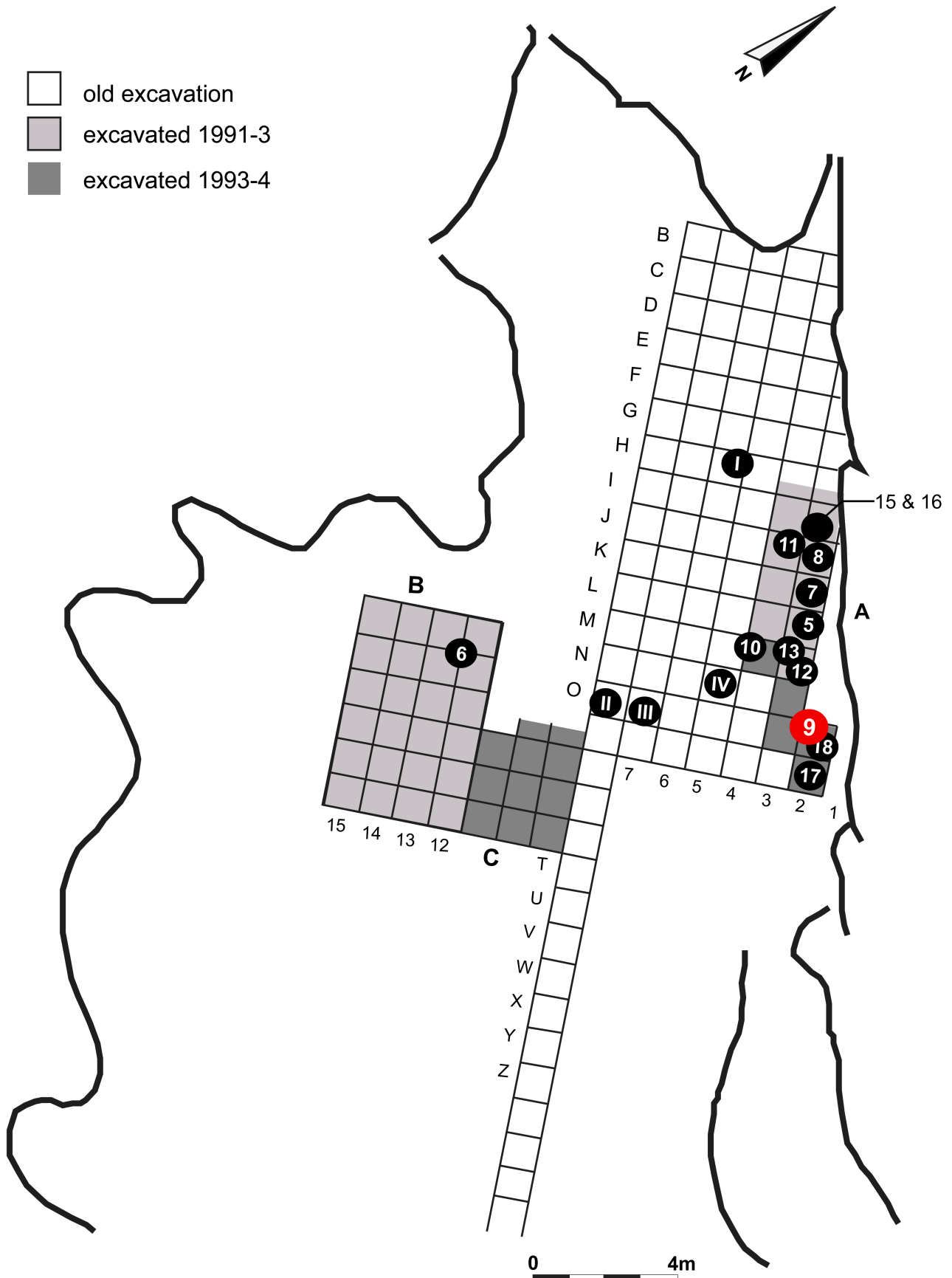


Figure 1. Excavations at Amud Cave.



Figure 2. Amud 9 fossils in situ.

Hovers and Belfer-Cohen 2013). The more recent analyses of the lithics do not support the hypothesis that the Amud assemblages are transitional.

#### CONTEXT OF THE AMUD 9 FOSSIL

The fossil remains from Amud Cave collected in 1991–1994 include Amud 9, a partial right distal leg and foot that preserves portions of the distal tibia, talus, first metatarsal, first proximal phalanx, a middle and distal phalanx of digit II–IV, and a sizable number of tiny, unidentifiable bone fragments that must have derived from the tibia, fibula, or other elements (Figure 2). Amud 9 was recovered at the end of the field season in 1993, when the bones were discovered protruding from the excavated profile, embedded in sediment underneath a large block (ca. 1.0m x 0.6m x 0.5m) of the cave's roof fall. The season was extended by a few days to allow safe removal of the hominin remains. The bones and the bottom of the fallen rock were separated by some 10cm of sediments containing Mousterian artifacts, suggesting that some time elapsed after the bones were deposited in the sediment and before the rock collapsed on top of them. Thus, neither death of the individual nor the burial of the bones are a direct result of the rock fall. When the block was removed no additional complete parts of a

skeleton were found beneath it. The sediment containing the foot bones was encased with plaster and the fossil was removed to the lab for delicate excavation.

The sediment surrounding Amud 9 contained many bone fragments, and Fourier-transform infrared spectroscopy of samples from the sediment beneath the rock refuted the hypothesis that the skeleton might have been lost to diagenesis (e.g., Weiner et al. 1993), since calcite ( $\text{CaCO}_3$ ), a more soluble mineral than bone mineral, was preserved below the block (Weiner, personal communication 1994; Hovers et al. 1995). Despite the time elapsed between bone deposition and rockfall (expressed by the amount of sediment covering the bones), the collapse of the large block from the roof may have completely pulverized all bone including hominin remains in an area of 3–4m<sup>2</sup> (Hovers et al. 1995), rendering the survival of the articulated foot fortuitous.

Excavation photographs of Amud 9 *in situ* (Figure 2) show several skeletal elements that later crumbled into small fragments and are now unsuitable for analysis. These lost elements include the distal fibula including the lateral malleolus, an additional metatarsal, that had a fairly long diaphysis and a relatively square base in superior view, and possibly the head of another metatarsal that lies about 1cm below the base of the first metatarsal. Enough of the other bones have survived that a substantial amount of comparisons and analysis are possible. The morphology and affinities of this specimen are the focus of this paper.

#### MATERIALS AND METHODS

A set of standard measurements (see Tables 2, 5, 8, 9, and 10 below) were made on the bones of Amud 9 with dial calipers by OMP in the Department of Anatomy, Sackler School of Medicine at Tel Aviv University, in 2012. Comparative data were drawn from a large set of measurements of fossil and recent tali and first metatarsals assembled by AP (Table 1; Arsuaga et al. 2015; Pablos 2013a, 2013b, 2017; Pablos et al. 2019a). Additional Neandertal tali from Shanidar 5 (Pomeroy et al. 2017) and El Sidrón (Rosas et al. 2017) were added to the data set but lacked one or more measurements that could be taken on Amud 9, and thus were excluded from the summary statistics in Tables 2 and 4 (see below). These tables include only specimens that preserved all of the measurements used in the discriminant analyses (see below). Comparative data for the hallux proximal phalanx and the intermediate and distal pedal phalanges were drawn from the literature (McCown and Keith 1939; Trinkaus 1975a, 1983; Trinkaus and Hilton 2006; Trinkaus and Shang 2008; Trinkaus et al. 2014; Vandermeersch 1981) or measured directly on Amud I, Qafzeh 8, and Qafzeh 9 by OMP during his study visit.

Since affinity to groups of fossil hominins is a key question for Amud 9, discriminant analyses were performed on measurements of the talus and then the first metatarsal of fossil and recent humans in order to create a discriminant space into which Amud 9 was subsequently interpolated. Statistical analysis was conducted using JMP 6.0 (SAS Institute, Cary, NC).

Additional points of interest are the estimation of body

TABLE 1. FOSSILS AND RECENT HUMANS USED FOR COMPARISONS.

	Talus	Metatarsal I
<b>Sima de los Huesos<sup>a</sup></b>	AT-860 (L), AT-965 (L), AT-966 (R), AT-980 (L), AT-1716 (L), AT-1822 (R), AT-1930 (R), AT-1931 (R), AT-2495 (R), AT-2803 (L), AT-3132 (L), AT-4425 (R)	
<b>Neandertals</b>	Kiik-Koba 1 (R) <sup>b</sup> , Krapina 235 (L) <sup>b</sup> , Krapina 236 (L) <sup>b</sup> , Krapina 237 (R) <sup>b</sup> , La Chapelle-aux-Saints (L) <sup>c</sup> , La Ferrassie 1 (R) <sup>c</sup> , La Ferrassie 2 (L) <sup>c</sup> , La Quina H1 (R) <sup>c</sup> , Le Régourdou 1 (R) <sup>c</sup> , Spy 2 (L) <sup>c</sup> , Tabun C1 (R) <sup>c</sup>	Gabasa (Ga1.Rev.439) (L) <sup>h</sup> , Kiik-Koba 1 (R) <sup>b</sup> , Krapina 245 (R) <sup>b</sup> , La Ferrassie 1 (L) <sup>c</sup> , La Ferrassie 2 (L) <sup>c</sup> , Shanidar 1 (L) <sup>i</sup> , Spy 25D (L) <sup>h</sup> , Tabun C1 (R) <sup>c</sup>
<b>Middle Paleolithic Modern Humans</b>	Qafzeh 3 (L) <sup>d</sup> , Qafzeh 8 (L) <sup>d</sup> , Qafzeh 9 (R) <sup>d</sup> , Skhul IV (L) <sup>e</sup> , Skhul V (L) <sup>f</sup> , Skhul VI (L) <sup>g</sup>	Qafzeh 3 (R) <sup>d</sup> , Qafzeh 8 (R) <sup>d</sup> , Skhul III (L) <sup>j</sup> , Skhul IV (L) <sup>k</sup>
<b>Upper Paleolithic</b>	Cro-Magnon 4337 (L) <sup>c</sup> , Cro-Magnon 4338 (R) <sup>c</sup> , Gough's Cave 1 (R) <sup>c</sup> , Abri Pataud 1 (R) <sup>c</sup>	Arene Candide 3 (L) <sup>l</sup> , Arene Candide 5 (R) <sup>l</sup> , Arene Candide 10 (R) <sup>l</sup> , Arene Candide 13 (L) <sup>l</sup> , Baoussou da Torre 1 (L) <sup>m</sup> , Cro-Magnon 4345-Bis (R) <sup>c</sup> , Gough's Cave 1 (R) <sup>c</sup> , Oberkassel 1 (L) <sup>n</sup> , Oetrange 1 <sup>o</sup> , Ohalo 2 (R) <sup>o</sup> , Abri Pataud 1 (R) <sup>c</sup> , Paviland 1 (R) <sup>p</sup> , Předmostí III (R) <sup>q</sup> , Tagliente 1 (R) <sup>r</sup>
<b>Recent Humans</b>	111 individuals from the Hamann-Todd Collection: 29 African American males <sup>c</sup> , 29 African American females <sup>c</sup> , 26 Euro-American males <sup>c</sup> , 27 Euro-American females <sup>c</sup>	194 individuals from the Hamann-Todd and AMNH collections: 40 African American females <sup>c</sup> , 40 African American males <sup>c</sup> , 54 Euro-American females <sup>c</sup> , 60 Euro-American males <sup>c</sup>

<sup>a</sup>Data from Pablos et al. (2013a).

<sup>b</sup>Data collected by Pablos from casts.

<sup>c</sup>Data collected by Pablos on the original specimens.

<sup>d</sup>Data from Vandermeersch (1981).

<sup>e</sup>Data from McCown and Keith (1939); Endo and Kimura (1970); and Trinkaus (1975a).

<sup>f</sup>Data from McCown and Keith (1939); Trinkaus (1975a); and Carlos Lorenzo, personal communication to Pablos.

<sup>g</sup>Data from McCown and Keith (1939); Trinkaus (1975a); Gambier (1981); and Carlos Lorenzo, personal communication to Pablos.

<sup>h</sup>Data from Carlos Lorenzo, personal communication to Pablos.

<sup>i</sup>Data from Trinkaus (1977, 1983).

<sup>j</sup>Data from McCown and Keith (1939); and Trinkaus (1975a).

<sup>k</sup>Data from McCown and Keith (1939).

<sup>l</sup>Data from Paoli et al. (1980).

<sup>m</sup>Data from Villotte et al. (2017).

<sup>n</sup>Data from Trinkaus (2015).

<sup>o</sup>Data from Trinkaus, personal communication to Pablos.

<sup>p</sup>Data from Trinkaus and Holliday (2000).

<sup>q</sup>Data from Matiegka (1938).

<sup>r</sup>Data from Corrain (1977).

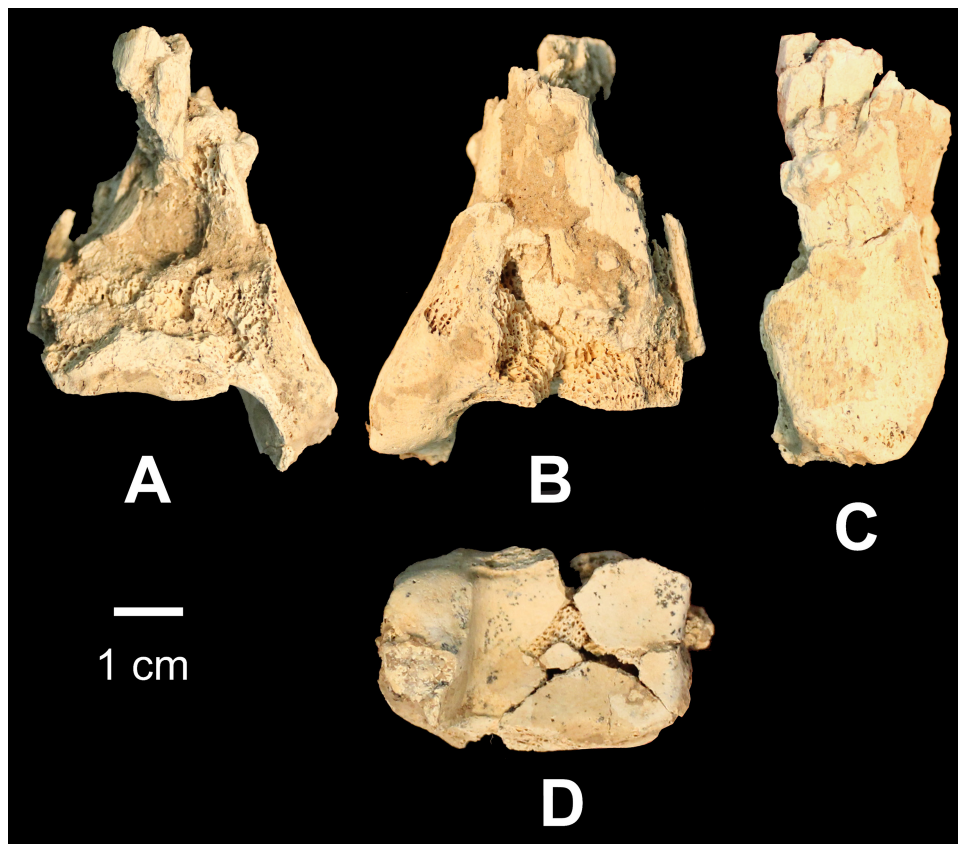


Figure 3. Right distal tibia of Amud 9: A) anterior; B) posterior; C) medial; D) inferior view (anterior is to the bottom).

mass and stature. Body mass was estimated from the formula for the width of the articular surface (M-5) of the talus published by McHenry (1992). Stature was estimated from formulae based on talus length and length (M-1a) of the first metatarsal (M-1) published by Pablos et al. (2013b). In order to provide a statistically informed estimate of the sex of Amud 9, we applied discriminant functions based on recent humans (Alonso-Llamazares and Pablos 2019).

## DESCRIPTIONS AND ANALYSIS

### LOST ELEMENTS

Between excavation and analysis, several bones of Amud 9 had disintegrated and are no longer suitable for analysis. Some measurements of the lost elements are possible, scaled relative to the scale bar visible in the photograph. Some of the elements appear to be slightly angled relative to standard anatomical planes, which will also distort the apparent measurements. Thus, the measurements based on the field photograph should be seen as approximate. The fibula measured 106mm from its distal end and the lateral malleolus maximum antero-posterior (AP) diameter of 29.7mm. The distal portion of the fibular diaphysis appears to be relatively narrow (11.4mm AP) just superior to the lateral malleolus, which flares slightly anteriorly and markedly posteriorly from the point of minimum thickness. The maximum length of the metatarsal I in the photograph is 56.6mm (versus 57.2mm on the actual bone), while the

length of the metatarsal II (or III?) is 71.6mm. The metatarsal II (or III) has a distal epiphysis breadth of 17.6mm, proximal epiphyseal breadth of perhaps 18.6mm (sediment partially covers one side), and a midshaft medio-lateral (ML) breadth of 9.4mm. Many of these dimensions are close to those of Tabun C1. McCown and Keith (1939) list (74.0mm) and 72.0mm for the total length of Tabun C1's right metatarsal II and III, respectively. These observations suggest that Amud 9 and Tabun C1 were roughly similar in size.

### DISTAL TIBIA

The distal tibia of Amud 9 comprises a crushed fragment that measures 68mm from superior to inferior (Figure 3). The distal articular surface is largely preserved but bears a series of small cracks that cross its surface, exposing cancellous bone superiorly. The anterior face of the distal epiphysis above the talar articular surface is preserved and bears a shallow fossa, the preserved portion of which measures 10.4mm wide by 4.7mm high. The fossa likely originally measured approximately 15mm in width and corresponds to a squatting facet (Boulle 2001a, 2001b; Trinkaus 1975b). The medial malleolus is largely preserved; it measures 13.7mm wide just distal to its junction with the distal articular surface. The ML breadth of the distal epiphysis (the projected distance from the most indented part of the rim of the notch to the medial-most point on the medial malleolus, measurement T9 of Pearson [1997]) measures 42.8mm; the corresponding measurement on Tabun C1 is 43.1mm and

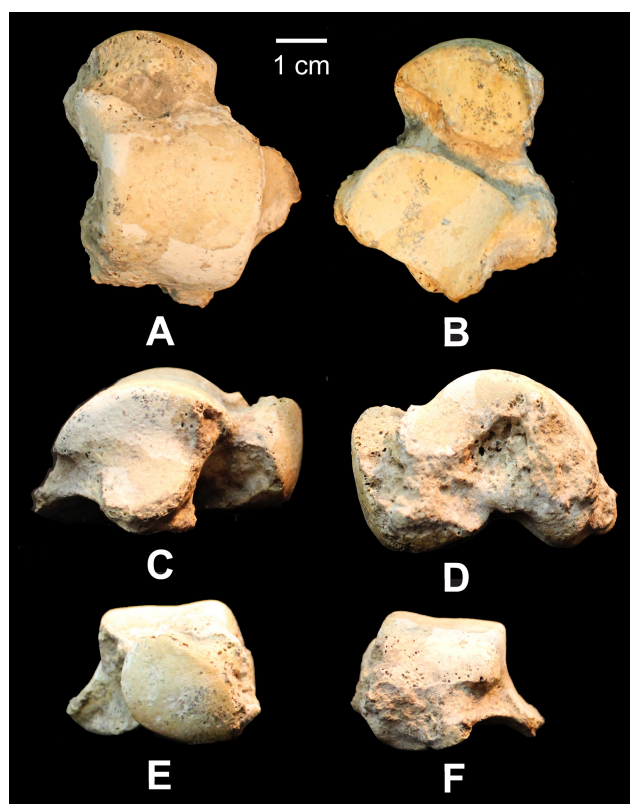


Figure 4. Right talus of Amud 9: A) superior; B) inferior; C) lateral; D) medial; E) anterior; F) posterior view.

that of La Ferrassie 2 is 43.2mm (Pearson 1997). Male Neandertals tend to have a wider distal epiphysis (52.2±2.9mm for five males (Pearson 1997). Been et al. (2017) report a slightly different measurement (maximum ML width of the distal epiphysis) of the right tibia of EQ3, a probable male, as 51.1mm. The same dimension is smaller, and similar in size to Amud 9, among the MP modern humans from Skhul, Qafzeh, and Omo Kibish (43.5±2.1mm; n=4; Pearson 1997), despite the fact that some of these early modern humans were notably taller than Neandertals (Carretero et al. 2012). The AP diameter of the distal epiphysis of Amud 9 cannot be reliably taken due to abrasion of the posterior side of the distal epiphysis.

Only small fragments that probably originally derived from distal fibula remain; these tiny fragments are too poorly preserved for analysis.

## TALUS

The right talus of Amud 9 is essentially complete (Figure 4; Table 2). It has a relatively short talar head and neck relative to the length of the trochlea, a small medial extension of the trochlear surface combined with a slight anterior extension of the articular surface for the medial malleolus (Barnett 1954; Trinkaus 1975a), a laterally flaring articular facet for the fibular malleolus, a fairly broad posterior portion of the trochlea that makes the medial and lateral edges of the trochlea seem almost parallel, and a projecting lateral lip of the groove for the tendon of the flexor hallucis

longus. Many of these features recall those of Neandertals as well as those of the hominins from Sima de los Huesos.

The distinctiveness of Neandertal tali relative to those of modern humans is well known (Pablos et al. 2012, 2013a, 2019a; Rhoads and Trinkaus 1977; Trinkaus 1975a, 1983). In general, Neandertals have a relatively short AP length of the talar head and neck relative to the length of the talar trochlea and a large, laterally projecting facet for the lateral malleolus (Gambier 1982; Pablos et al. 2013a; Rhoads and Trinkaus 1977; Trinkaus 1983). Rosas et al.'s (2017) geometric morphometric analysis of Neandertal tali from El Sidrón corroborates previous observations of the Neandertal pattern of morphology but adds interesting new details—the shortness of the neck and head is not due to lengthening of the trochlea in proportion to the combined length of both. The expansion of the trochlea involves both of its articular facets, the medial trochlear facet shows more anterior curvature than modern humans, the medial and lateral trochlear rims are more equal, and the calcaneal facet has a notably large lateral extension. The analysis of the hominin tali from the Middle Pleistocene site of Sima de los Huesos demonstrates that, in comparison to most recent humans, they share a proportionately short head plus neck and laterally projecting articular facet for the lateral malleolus (a trait that is even more exaggerated in Sima de los Huesos than in Neandertals), and a relatively wide posterior portion of the trochlea (Arsuaga et al. 2015; Pablos et al. 2013a, 2017). However, Neandertals tend to have a ML wide head of the talus in comparison to modern humans, while tali from Sima de los Huesos tend to have a head that is proportionately narrow ML relative to modern humans and even more so relative to Neandertals (Pablos et al. 2013a, 2017).

The sub-talar joints of Amud 9 feature a relatively large, posterior calcaneal facet that is bounded an inferiorly projecting edge on its lateral side. The sulcus tali is deep and fairly wide, possibly indicating a strong talocalcaneal ligament. The medial and anterior calcaneal facets on the inferior surface of the neck and head are fused into a single facet shaped like a comma with its tail tapering along the antero-medial side of the inferior edge of the head. Amud 9's junction between the anterior and medial facets forms a gentle curve rather than a distinct angle. Fusion of these facets is common in Neandertals, occurring in Shanidar 1, Amud I, Shanidar 5, and in 89.7% of a pooled sample 29 Neandertal tali (Pablos et al. 2012; Pomeroy et al. 2017; Rosas et al. 2017; including 2 of 4 observable El Sidrón tali as having completely fused facets), and 100% of 17 observable tali from Sima de los Huesos (Pablos et al. 2012, 2013a). Fusion of the facets is also common but less frequent in samples of recent humans, who have frequencies ranging between 55–75% (Pablos et al. 2012; Pomeroy et al. 2017; Trinkaus 1975a).

Body mass was estimated from the breadth of the talar trochlea (M-5; McHenry 1992). In the case of Amud 9, the value for M-5 is 26.8mm, which provides an estimate of 59.9kg -7.7/+8.9kg (52.2–68.8kg [±1 standard deviation range]) for the individual.

Based on the best-fit regression formula published by

TABLE 2. MEASUREMENTS OF THE TALUS.

Martin number*	Description	Amud 9	Neandertals (n= 12)	MPMH (n= 6)	UP (n= 4)	Recent (n=111)	SH (n=12)
M1	Talar Length	48.2	50.7±3.6	53.3±4.1	51.9±3.4	52.8±4.0	51.8±3.6
M1a	Total length	53.9	--	--	--	--	--
M2	Total breadth	38.6	44.6±4.3	44.1±2.7	43.5±1.8	40.7±3.6	41.9±3.6
M3	Talar height	27.3	31.0±3.3	32.3±1.3	30.8±1.2	29.0±4.0	29.3±2.6
M4	Trochlear length	30.0	33.1±3.4	34.7±1.8	33.2±2.0	33.0±2.7	32.7±2.2
M5	Width of the trochlea	26.8	28.8±2.2	28.4±3.0	29.5±1.8	29.4±2.6	29.5±1.8
M5(1)	Posterior width of the trochlea	25.6	26.6±2.6	25.3±4.3	25.9±1.9	26.0±2.5	27.5±1.9
M5(2)	Anterior width of the trochlea	26.1	--	--	--	--	--
M6	Height of the trochlea	13.3	--	--	--	--	--
M8	Length of the head and neck	13.8	19.4±1.9	19.2±2.5	22.1±1.4	23.1±2.9	20.2±1.4
M9	Length of the neck	30.1	34.7±3.7	33.6±3.5	34.2±3.0	32.5±3.0	30.5±2.3
M10	Width of the neck	20.8	22.9±2.1	22.6±2.4	22.4±1.3	22.8±2.0	22.3±1.7
M11	Height of the neck	5.1	--	--	--	--	--
M12	Length of the posterior calcaneal articular surface	27.4	31.4±3.1	32.8±3.0	33.1±1.8	31.0±2.8	31.7±1.9
M13	Width of the posterior calcaneal articular surface	21.8	22.3±1.8	22.9±1.7	21.6±2.4	21.3±2.1	21.4±1.4
M16	Angle of the neck	16°	--	--	--	--	--
M17	Angle of torsion of the head	45°	--	--	--	--	--
M17a	Angle of torsion	36°	--	--	--	--	--

\*Martin numbers refer to measurements defined by Martin and Saller (1957) and revised by Bräuer (1988).

Abbreviations: MPMH, Middle Paleolithic modern humans (Skhul, Qafzeh, and Omo Kibish I); UP, European Upper Paleolithic; SH, Sima de los Huesos. Samples are described in Table 1.

Pablos et al. (2013b), which was constructed based on the pooled sample of recent females, the predicted stature for Amud 9 based on the maximum length (M-1a) of its talus is  $163.4 \pm 4.7$  cm.

In order to determine which hominins Amud 9's talus most closely resembles, we performed a discriminant analysis on 11 talar measurements on five groups (sexes pooled in each)—recent humans, Upper Paleolithic (UP) individuals, Middle Paleolithic modern humans (MPMH), Neandertals, and Sima de los Huesos (Table 3). Amud 9 was initially excluded from the analysis, which defined a discriminant space that separated the groups in the analysis. Amud 9 was then interpolated into this discriminant space (Figure 5). The discriminant analysis most clearly separates recent humans from more ancient humans, including Neandertals, MP modern humans, and Sima de los Huesos. Table 4 presents the posterior classifications for individuals in the analysis with between 50% to 100% of the individuals in each sample classified correctly. The appreciable number

of mis-assignments among Neandertals, MP Modern Humans, and Sima de los Huesos reinforces the impression of the general similarities among these three groups.

With regard to the variables responsible for separating groups, on the first canonical axis, measurement M2 (width, which includes both the trochlea and the facet for the lateral malleolus, both of which tend to be large in the ancient specimens) is most clearly associated with these differences, while measurement M5-1 (breadth of the posterior part of the trochlea) plays an important role in pushing specimens from Sima de los Huesos away from recent and UP humans on canonical axis 2. Amud 9 is located in the lower right quadrant of the plot of individual scores on axes 1 and 2 (see Figure 5), falling closest to Sima de los Huesos. The closest *post hoc* group assignment of Amud 9 is to Sima de los Huesos ( $p=0.76$ ), followed by MP Modern Humans (Skhul-Qafzeh;  $p=0.12$ ) and Neandertals ( $p=0.11$ ). The assignment of Amud 9 to Sima de los Huesos is largely driven by its large width of the posterior part of the troch-

TABLE 3. DETAILS OF THE DISCRIMINANT ANALYSIS OF THE TALUS.

	Axis 1	Axis 2	Axis 3
<b>Eigenvalue:</b>	1.3154	0.3076	0.1209
<b>Percent variance:</b>	72.97	17.06	6.71
<b>Cumulative percent:</b>	72.97	90.04	96.75
	Eigenvector 1	Eigenvector 2	Eigenvector 3
<b>M1</b>	-0.1327	-0.3298	-0.3256
<b>M2</b>	0.4390	0.0241	0.0240
<b>M3</b>	0.0435	0.0485	-0.0144
<b>M4</b>	-0.0581	0.1655	-0.0894
<b>M5</b>	-0.1727	0.0065	0.1517
<b>M5-1</b>	0.1181	-0.2951	0.3645
<b>M8</b>	-0.3028	0.2797	0.1315
<b>M9</b>	0.0700	0.4082	0.1019
<b>M10</b>	-0.1397	-0.0335	0.0469
<b>M12</b>	-0.0504	-0.0509	-0.1935

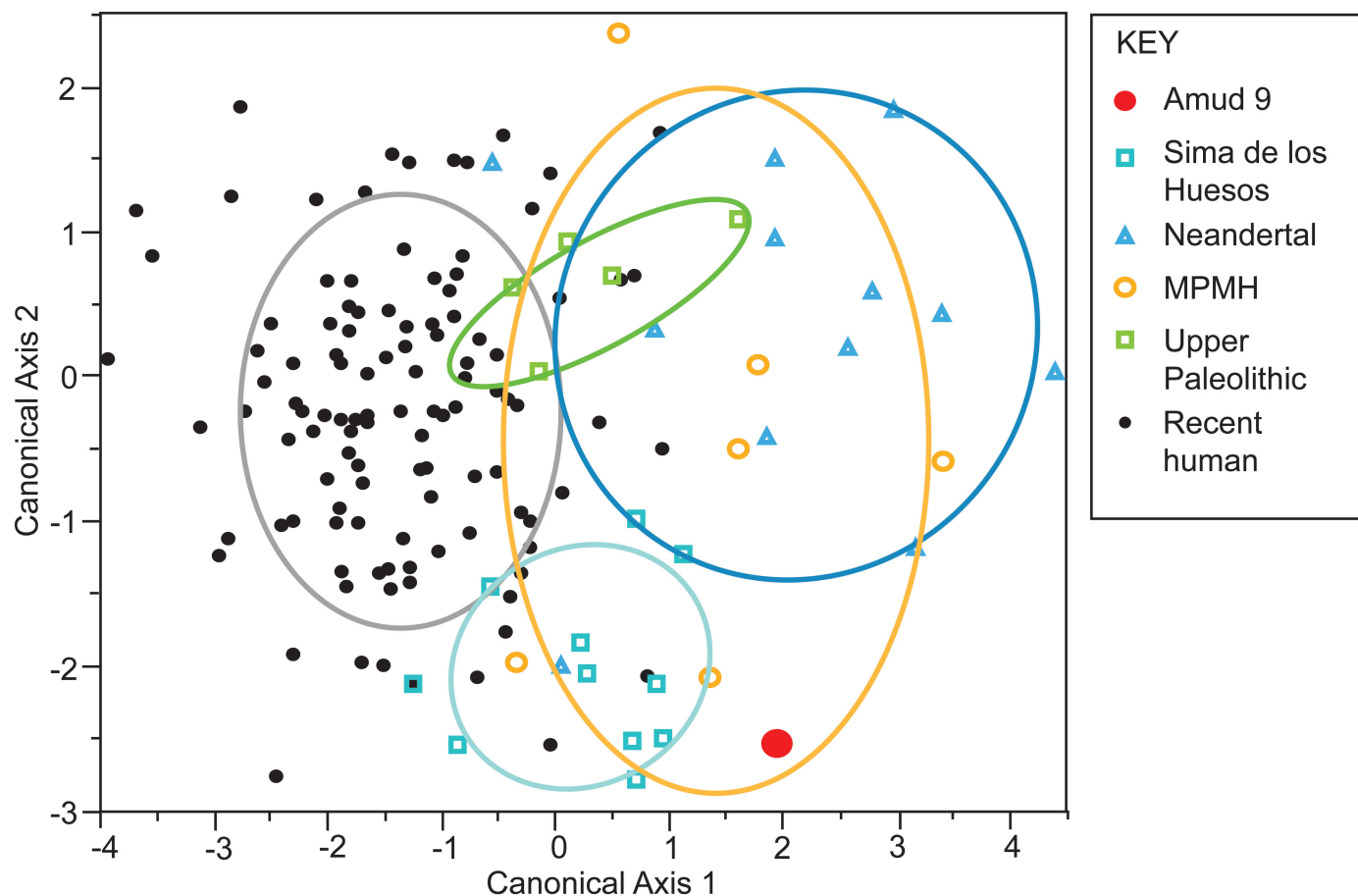


Figure 5. Discriminant analysis of the talus (raw data). A 67% density ellipse surrounds each group's centroid. MPMH stands for Middle Paleolithic modern humans.

**TABLE 4. POSTERIOR GROUP ASSIGNMENTS FROM THE CVA ON THE TALUS (raw data).\***

Actual rows by assigned columns	MPMH	Neandertals	Recent	SH	UP
<b>MPMH</b>	3 (50%)	1 (16.7%)	0 (0%)	2 (33.3%)	0 (0%)
<b>Neandertals</b>	2 (11.8%)	10 (58.8%)	0 (0%)	2 (11.8%)	3 (17.6%)
<b>Recent</b>	3 (2.7%)	2 (1.8%)	83 (74.8%)	10 (9%)	13 (11.7%)
<b>SH</b>	0 (0%)	0 (0%)	0 (0%)	12 (100%)	0 (0%)
<b>UP</b>	0 (0%)	0 (0%)	1 (20%)	0 (0%)	4 (80%)
<b>Amud 9</b>	20.83%	7.31%	0.37%	71.36%	0.14%

\*The data in each cell show the number of tali assigned to the groups indicated in each column followed in parentheses by the percentage of individuals in the row. The values for Amud 9 show posterior probabilities of its assignment to each group. Abbreviations: MPMH, Middle Paleolithic Modern Humans; SH, Sima de los Huesos; UP, Upper Paleolithic.

lea (M5-1), which loads heavily on canonical axis 3 (see Table 3). It must be noted that canonical axis 3 accounts for only 6.71% of the between-group variance.

The assignment of Amud 9's talus to Sima de los Huesos was unexpected. We checked the effect of Sima de los Huesos fossils in the discriminant analysis by re-running the analysis without Sima de los Huesos (results not shown). Discrimination between the other groups remained similar, again emphasizing the role of M2 (width) in separating ancient from recent humans. With Sima de los Huesos removed, however, Amud 9's interpolation into discriminant space showed it had the highest probability of being a Neandertal ( $p=0.60$ ), followed closely by the likelihood of being a MP modern human ( $p=0.40$ ). The conclusion from these analyses is that Amud 9 has a talus that broadly resembles Neandertals and the earlier hominins from Sima de los Huesos (Arsuaga et al. 2014), as well as the MP modern human sample, which largely comprises fossils from Skhul and Qafzeh. The wide posterior breadth of the trochlea may simply be a manifestation of idiosyncratic variation rather than a clear taxonomic signal.

To check the possibility (raised by a reviewer of this paper) that the size—as measured by the geometric mean of the variables used in the CVA—of the talus determined the taxonomic attributions, we plotted the geometric means of specimens used in the analysis versus their positions on canonical axis 2 and axis 2 (Figure A1 in the Appendix). The results showed that Amud 9's talus is indeed small, but the geometric means of tali are uncorrelated with positions on either axis. There are large and small tali in all of the groups with substantial sample sizes.

We re-ran the discriminant analysis using shape variables, in which each measurement was divided by the geometric mean of the 11 variables for that individual (Darroch and Mosimann 1985; Mosimann 1970). In common with our previous experiences in performing the same analysis on raw and shape data (Churchill et al. 1996; Pearson 1997), the analysis of shape data produced results that are quite similar to those from the raw data (Appendix, Figure A-2, Tables A-1 and A-2). However, one difference that could be important in the present context is that the analysis of shape data predicted Amud 9 to be a MP Modern Human

(posterior probability=88.53%), followed more distantly by an affinity to Neandertals (posterior probability=10.03%). The close relationship between Amud 9 and Sima de los Huesos (SH) disappears (posterior probability of membership in SH=1.44%).

Despite the limitations involved in assigning sex to fossil populations, and although there are no associated pelvic remains, we tried to make an approximate assignment to sex of Amud 9 based on talus dimensions using the two sets of discriminant functions provided by Alonso-Llamazares and Pablos (2019). First, we applied the best univariate formula for sex estimation for the talus, which uses talar length (M1), the dimension associated with the greatest accuracy of prediction in the recent sample used to construct the discriminant formulae. Second, we estimated the sex with a stepwise formula using five variables—talar length (M1), trochlear height (M6), trochlear length (M4) and the length and breadth of the calcaneal posterior articular surface (M12 and M13). Both discriminant analyses identified Amud 9 as a female, with 90.2% accuracy for talar length and 93.8% accuracy for the stepwise regression. Both estimates of the accuracy are made for the recent human sample used to create the discriminant analyses, so additional caution is required in accepting these results for Neandertals. Nevertheless, the discriminant analyses support the impression that Amud 9's foot came from a fairly small, and probably female, individual.

#### FIRST METATARSAL

Amud 9's right metatarsal I is almost complete except for some abrasion on the lateral and especially the medial aspect of the plantar quarter of the proximal articular surface of the base (Figure 6) and additional taphonomic abrasion that has destroyed the articular facet for metatarsal II on the lateral side of the base. Measurements and comparative data for Amud 9's metatarsal I appear in Table 5. Dimensions of lateral articular facet for the base of metatarsal II cannot be recorded due to damage to the lateral side of the proximal epiphysis.

Neandertal metatarsals, including the first, tend to be relatively short and broad compared to those of recent humans (Pablos et al. 2012; Pablos et al. 2017; Pearson and

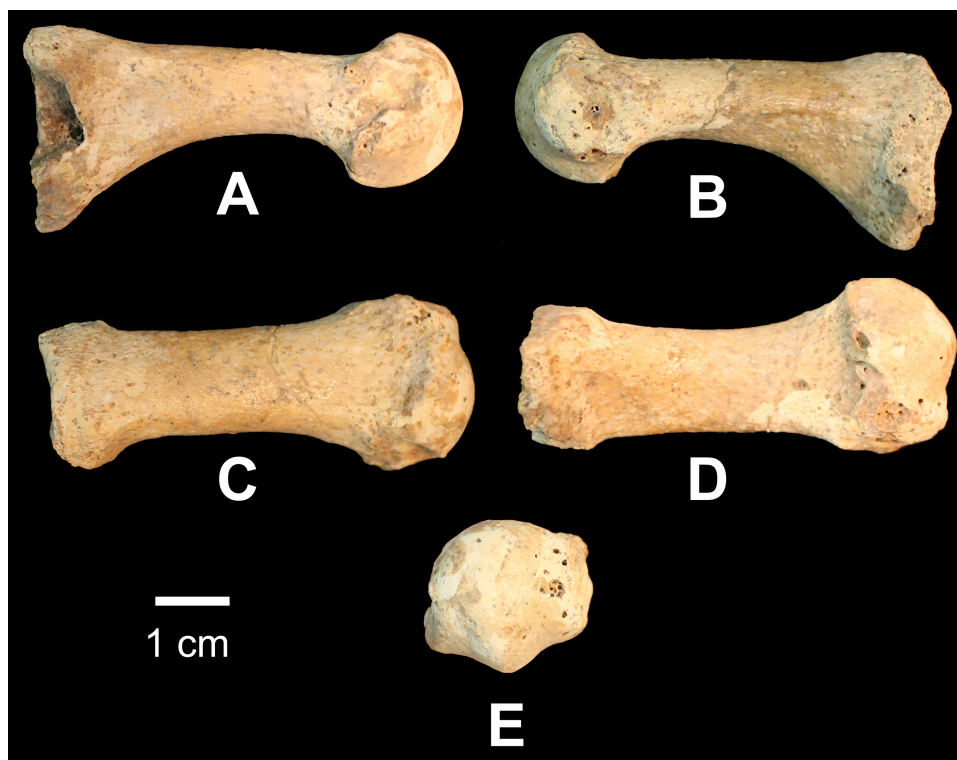


Figure 6. Right first metatarsal of Amud 9: A) lateral; B) medial; C) superior; D) inferior; E) distal view.

**TABLE 5. MEASUREMENTS OF THE FIRST METATARSAL.**

Martin number	Description	Amud 9	Neandertals (n = 8)	MPMH (n = 4)	UP (n = 15)	Recent (n = 194)
M1b	Articular length	57.2	60.3±5.9	61.5±2.8	63.2±6.0	62.9±4.6
M1	Maximum length	58.9	--	--	--	--
M3	Medio-lateral width at midshaft	14.1	14.6±1.7	15.5±1.3	13.6±1.6	13.1±1.6
M4	Dorso-plantar height at midshaft	11.5	12.5±2.0	14.3±0.6	13.7±1.6	13.8±1.5
M6	Proximal medio-lateral width	18.7	21.4±3.1	21.1±1.7	20.4±3.1	20.3±2.0
M7	Proximal dorso-plantar height	27.5	30.4±4.5	29.4±0.7	29.1±2.3	29.0±2.2
M8	Distal medio-lateral width	21.6	23.5±2.6	23.1±1.1	22.3±1.5	21.7±2.0
M9	Distal dorso-plantar height	20.3	21.4±2.7	20.1±1.0	21.8±1.4	19.9±1.9

Abbreviations: MPMH, Middle Paleolithic Modern Humans, UP, Upper Paleolithic, SH, Sima de los Huesos.

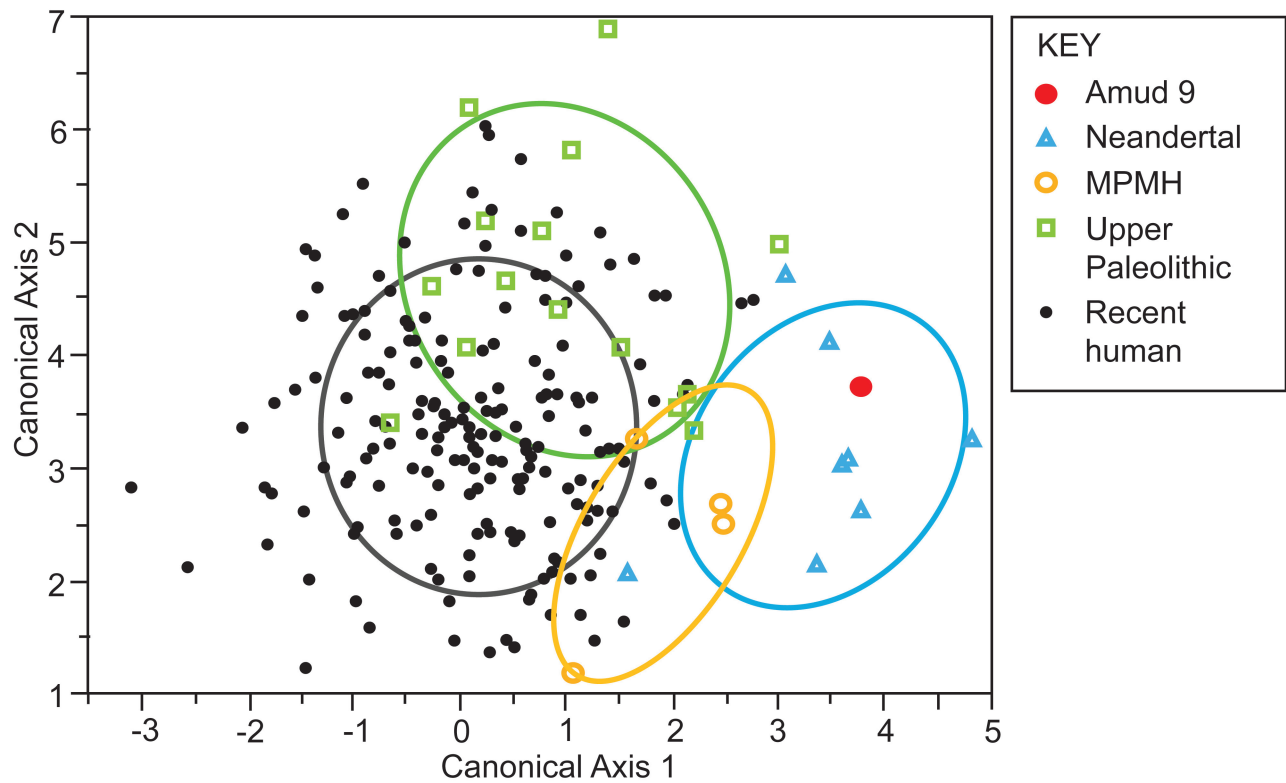


Figure 7. Discriminant analysis of the metatarsal (raw data). A 67% density ellipse surrounds each group's centroid. MPMH stands for Middle Paleolithic modern humans.

Busby 2006), a pattern that mirrors the trend in most of their other long bones and likely reflects ecogeographic variation as well as vigorous use in life (Pearson 2000a, 2000b).

An estimate of stature based on the regression formulae using the maximum length of the first metatarsal (58.9mm for Amud 9) was made using Pablos et al.'s (2013b) formula for their pooled sample of recent Euro-American and African-American females. This yields an estimate of  $160.6 \pm 2.8$  cm for Amud 9. Pablos et al. (2013b) also published a formula for stature that includes M1a from the talus and M1 of the first metatarsal. Using both dimensions, the formula based on the pooled group of recent females yields an estimate of  $159.7 \pm 2.6$  cm for Amud 9's stature.

In order to assess the overall affinities of Amud 9's metatarsal I to fossil and recent humans, we ran a discriminant analysis based on seven measurements that could be taken on the individuals listed in Table 1. Amud 9 was initially excluded, then interpolated into the discriminant space that separated recent humans, UP Europeans, MP Modern Humans, and Neandertals. No first metatarsals from Sima de los Huesos could be included since measurements of them have not yet been published. In the resulting analysis (Figure 7; Table 6), Amud 9 clearly falls with Neandertals on the first canonical axis, which accounts for 70.3% of between-group variance (see Figure 7). Positions on the right of Axis 1 (among the Neandertals) are largely driven by large values for M3 (width at midshaft) and to a lesser extent by M7 (dorso-plantar diameter of the proxi-

mal epiphysis) and M8 (width of the distal epiphysis), all of which tend to be relatively large in Neandertals and Amud 9. The analysis does a reasonably good job of classifying first metatarsals (Table 7), with correct classifications ranging from 60.9% for UP individuals to 87.5% for Neandertals. Amud 9 was classified as a Neandertal (posterior probability=81.76%) with the next highest likelihood of being a MP Modern Human (posterior probability=15.01%).

We repeated the discriminant analysis on the first metatarsal using shape data (Appendix Figure A-3, Tables A-3 and A-4) and found a very similar pattern. Amud 9 again is classified as a Neandertal (posterior probability=89.57%), followed more distantly by a MP Modern Human (posterior probability=8.35%).

### PROXIMAL PEDAL PHALANX I

The right proximal pedal phalanx of Amud 9 is complete with the exception of the distal portion of the medial condyle, which was lost postmortem (Figure 8). A small mass of adhering matrix obscures the distal part of the plantar surface just proximal to the medial epicondyle. The proximal and preserved portion of the distal articular surfaces appear healthy. Measurements and comparative data appear in Table 8.

Neandertal first proximal pedal phalanges tend to be absolutely short and relatively broad, but with overlap of the variation present in early modern humans as well as living people (Pablos et al. 2019a; Trinkaus 1975a, 1983).

**TABLE 6. DETAILS OF THE DISCRIMINANT ANALYSIS OF THE METATARSAL (raw data).**

	Axis 1	Axis 2	Axis 3
<b>Eigenvalue:</b>	0.4478	0.1322	0.0566
<b>Percent variance:</b>	70.3	20.8	8.9
<b>Cumulative percent:</b>	70.3	91.1	100.0
	Eigenvector 1	Eigenvector 2	Eigenvector 3
<b>M1</b>	-0.1490	0.0943	0.0310
<b>M3</b>	0.8311	-0.0999	-0.6924
<b>M4</b>	-0.812	-0.0257	-0.5495
<b>M6</b>	-0.3640	-0.0997	0.3473
<b>M7</b>	0.4031	-0.2944	0.4154
<b>M8</b>	0.0864	-0.3251	-0.0133
<b>M9</b>	0.1836	0.8374	-0.0481

Comparison with Skhul and Qafzeh reveals that Neandertal specimens tend to have similar breadths but shorter absolute lengths. It is interesting in this regard that Amud 9's first proximal pedal phalanx is relatively long relative to the width of its base (Figure 9). This departs from the usual Neandertal morphology and resembles the condition in modern humans. This longer shaft may, however, simply reflect the primitive morphology, perhaps inherited as a polymorphic state by Levantine Neandertals from their Middle Pleistocene ancestors. If so, it may not necessarily represent a trait that could only have been inherited from admixture with anatomically modern humans.

#### INTERMEDIATE PEDAL PHALANX

The intermediate pedal phalanx of Amud 9 is complete and well preserved (Figure 10; Table 9). A small encrustation of adhering matrix and crushed bone, measuring 5.2mm long proximo-distally by 5.6mm wide, covers much of the plantar surface of the diaphysis, and prevents an accurate measurement of the dorsal-plantar height at midshaft. The phalanx is short and relatively broad throughout its length.

It generally resembles other Neandertal intermediate pedal phalanges from digit II-IV. It is very close in size to Tabun C1's intermediate pedal phalanx II (see Table 9), and also may be from the second digit. However, among the few Neandertals that preserve several intermediate pedal phalanges (e.g., La Ferrassie 1, La Ferrassie 2, Kiik-Koba 1, and Shanidar 4), there is often only a small difference in size between digits II and III and sometimes IV as well (data in Trinkaus 1975a). Furthermore, as Trinkaus has observed (1975a, 1983), the diaphyses of pedal phalanges of digits IV and V of Neandertals tend to show much less decrease in breadth relative to digits II and III than do the toes of many modern humans. This robusticity of the lateral proximal pedal phalanges forms a central piece of evidence that supports the hypothesis that Neandertals and MP modern humans may not have worn footwear (Trinkaus and Hilton 2006; Trinkaus and Shang 2008). Relatively high robusticity of the lateral pedal rays also characterizes the foot bones from Sima de los Huesos (Arsuaga et al. 2015). As a result, the assignment to a specific ray of Amud's intermediate pedal phalanx remains difficult.

**TABLE 7. POSTERIOR GROUP ASSIGNMENTS FROM THE CVA ON THE FIRST METATARSAL (raw data).\***

Actual rows by assigned columns	MPMH	Neandertals	Recent	UP
<b>MPMH</b>	3 (75%)	1 (25%)	0 (0%)	0 (0%)
<b>Neandertals</b>	1 (12.5%)	7 (87.5%)	0 (0%)	0 (0%)
<b>Recent</b>	17 (8.8%)	4 (2.1%)	140 (72.2%)	33 (17.0%)
<b>UP</b>	1 (6.7%)	3 (13.0%)	5 (21.7%)	14 (60.9%)
<b>Amud 9</b>	15.01%	81.76%	0.27%	2.96%

\*The data in each cell show the number of tali assigned to the groups indicated in each column followed in parentheses by the percentage of individuals in the row. The values for Amud 9 show posterior probabilities of its assignment to each group. Abbreviations: MPMH, Middle Paleolithic Modern Humans; SH, Upper Paleolithic.

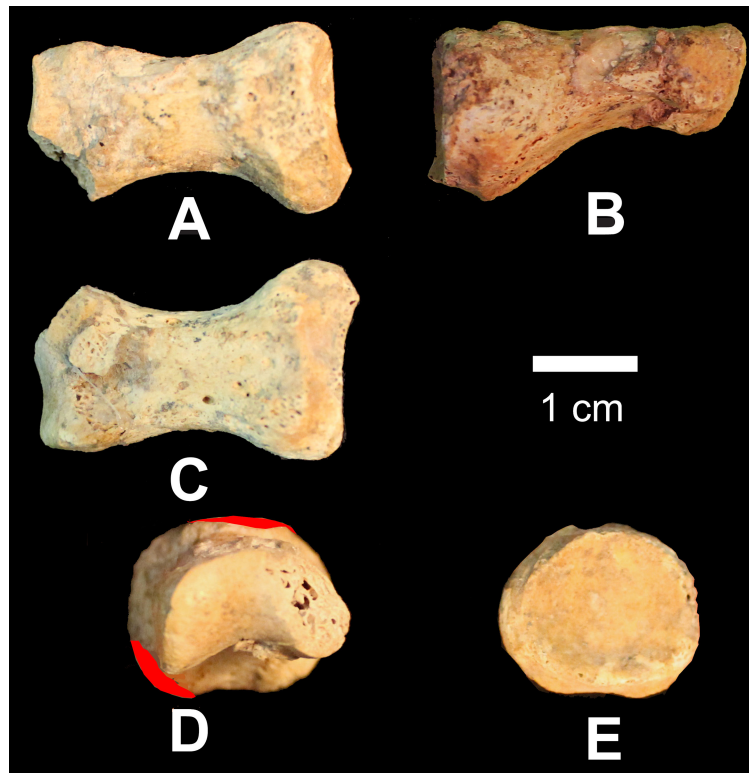


Figure 8. Right proximal pedal phalanx I of Amud 9: A) superior; B) medial; C) inferior; D) distal (red indicates area hidden by supports in the original photograph); E) proximal view.

### DISTAL PEDAL PHALANX

The distal pedal phalanx of Amud 9 is also an absolutely short and relatively broad bone. It has a wide apical tuft and a relatively broad base (see Figure 10; Table 10). It is fairly symmetrical around its long axis and shows very little sign of medial deflection of its long axis relative to the base. These features make it much more likely that the distal phalanx belongs to digits II or III rather than IV or V (Pablos et al. 2019b). The proximal, medial side of plantar surface is partially covered by an adhering mass of pulverized bone and matrix measuring 6.3mm long proximo-distally by 5.2mm ML. The fossil resembles the distal pedal phalanges II-IV, and most closely those of digits II-III, of Neandertals (see Table 10). Its closest match is the right distal pedal phalanx II of Tabun C1 (see Table 10).

### DISCUSSION

We interpret Amud 9 as a Neandertal and clearly distinct from UP and recent modern human foot bones. However, other interpretations are possibly supported by the substantial overlap in talar morphology between Skhul-Qafzeh hominins and Neandertals. A possible source of the similarity in talar shapes between Neandertals and Skhul-Qafzeh could be admixture<sup>1</sup> between MP modern humans and Neandertals that predates the 50–70 ka exodus from Africa. A trace ( $\leq 2\%$ ) of such admixture may be present in Altai Neandertals (Kuhlwilm et al. 2016). At present, however, claims that archaic morphology in the Skhul and Qafzeh hominins must have resulted from admixture with Nean-

dertals remain speculative and are inconsistent with the evidence from dental morphology that refutes the hypothesis of a substantial Neandertal admixture in the Skhul-Qafzeh sample (Bailey et al. 2017).

A problem that complicates interpretation of the morphological patterns in the Near Eastern Neandertals is the fact that they display a substantial amount of morphological variability. Admixture from early modern humans certainly might account for this variability<sup>1</sup>, but so might a larger, less bottlenecked population among the Near Eastern Neandertals than among their European kin, especially those from MIS 3 (Dalén et al. 2012). Long ago, Howell (1957) argued that population bottlenecks could be a viable explanation for some of the observed differences among Neandertals, including those from the Last Interglacial site of Krapina and later, Western European “classic” Neandertals.

Examples of the high degree of morphological variation in Near Eastern Neandertals include Dederiyeh 1 and 2, two juveniles, both around 2 years of age relative to standards of growth and development for modern children, who differ strongly in terms of their physique. Dederiyeh 1 is massively built (Kondo and Dodo 2002) while Dederiyeh 2 has more slender long bones (Kondo and Ishida 2002). McCown and Keith’s (1939) description of Tabun C1 indicates that she was fairly small and had slender long bones combined with almost a full suite of other Neandertal traits. Tillier (2005) reviewed the stratigraphic problems in associating the Tabun C1 burial with Level B (which argu-

TABLE 8. MEASUREMENTS OF THE PROXIMAL PEDAL PHALANX I.

Martin number	Description	Amud 9	Neandertals <sup>b</sup>	MPMH <sup>c</sup>	SH <sup>d</sup> (n = 8)
M1	Maximum length	(30.7) <sup>a</sup>	--	36.2±1.3 (n=3)	34.1±1.4 (n=7)
M1a	Articular length	26.9	25.7±2.0 (n=5)	32.2±0.7 (n=3)	--
M3a	Dorso-plantar height of the base	15.5	17.1±1.8 (n=6)	17.0 (n=1)	--
	Dorso-plantar height of the proximal articular surface	13.2	14.4±1.0 (n=5)	--	--
M2a	Medio-lateral width of the base	18.4	19.8±2.2 (n=6)	20.8 (n=1)	--
	Medio-lateral width of the proximal articular surface	15.2	18.0±1.7 (n=5)	--	--
M3	Midshaft dorso-plantar height	9.5	9.7±1.2 (n=4)	9.6±0.1 (n=2)	--
M2	Midshaft medio-lateral width	11.0	13.1±0.8 (n=4)	13.2±0.5 (n=2)	14.0±1.6
M3b	Dorso-plantar height of the distal articular surface	9.2	9.4±0.6 (n=4)	10.0±1.6 (n=3)	--
M2b	Medio-lateral width of the distal articular surface	-- <sup>a</sup>	17.1±0.9 (n=4)	16.6±0.4 (n=3)	--
--	Radius of curvature <sup>e</sup>	127.4			
	Included angle <sup>e</sup>	6.36°			

Abbreviations: MPMH, Middle Paleolithic Modern Humans, UP, Upper Paleolithic, SH, Sima de los Huesos.

<sup>a</sup>Damage to medial condyle.

<sup>b</sup>Neandertal sample: Tabun C1 (R) (McCown and Keith 1939); Shanidar 1 (L), 3 (R?), 4 (R), and 8 (R) (Trinkaus 1983); La Ferrassie 2 (R) (Vandermeersch 1981).

<sup>c</sup>MPMH sample: Qafzeh 6 (R), 8 (R), and 9 (R) (Vandermeersch 1981); Skhul IV (R) (McCown and Keith 1939).

<sup>d</sup>Data from Pablos et al. (2017) and the supplementary information in Arsuaga et al. (2015).

<sup>e</sup>Following Susman et al. (1984).

ably would make the burial contemporaneous with the Neandertals from Kebara) or Level C (which would arguably make it roughly contemporaneous with Skhul and Qafzeh). She noted that in addition to a low body mass for stature, the Tabun C1 skeleton retains primitive features such as a receding mandibular symphysis, projecting supraorbital torus, and low cranial capacity, which might combine to suggest that this individual belonged to a morphologically more primitive grade of Neandertals that she thought would have preceded those from Kebara and Amud. Endo and Kimura (1970) noted that Amud I was relatively tall and slender in comparison to Neandertal males from Europe. Amud I also has a relatively unbowed radial shaft (Endo and Kimura 1970), as do Shanidar 1 and 6 (Trinkaus 1983). Kebara 2 has a distinctive pelvis relative to modern humans (Rak 1990, 1991; Rak and Arensburg 1987). Nean-

dertals inherited many aspects of this pelvic morphology from a Middle Pleistocene ancestor (Arsuaga et al. 1999, 2015). Kebara 2 has almost the full suite of Neandertal features in its upper limb (Vandermeersch 1991). Arensburg (1991) argued that many features of the vertebral column show overlap with modern humans, but Gómez-Olivencia et al.'s (2009, 2018) re-evaluation of the vertebrae and ribs showed clear differences with recent humans and likely reflected a wide, capacious thorax that was associated with a wide body plan and likely was inherited from Middle Pleistocene *Homo* or perhaps even *Homo erectus* (Arsuaga et al. 1999; Simpson et al. 2008). Likewise, Been et al. (2010, 2017a) demonstrated that Kebara 2's lumbar vertebrae have transverse processes that differ in orientation from the usual morphology in recent humans. The lower limb bones of the probable young male Neandertal from 'Ein Qashish

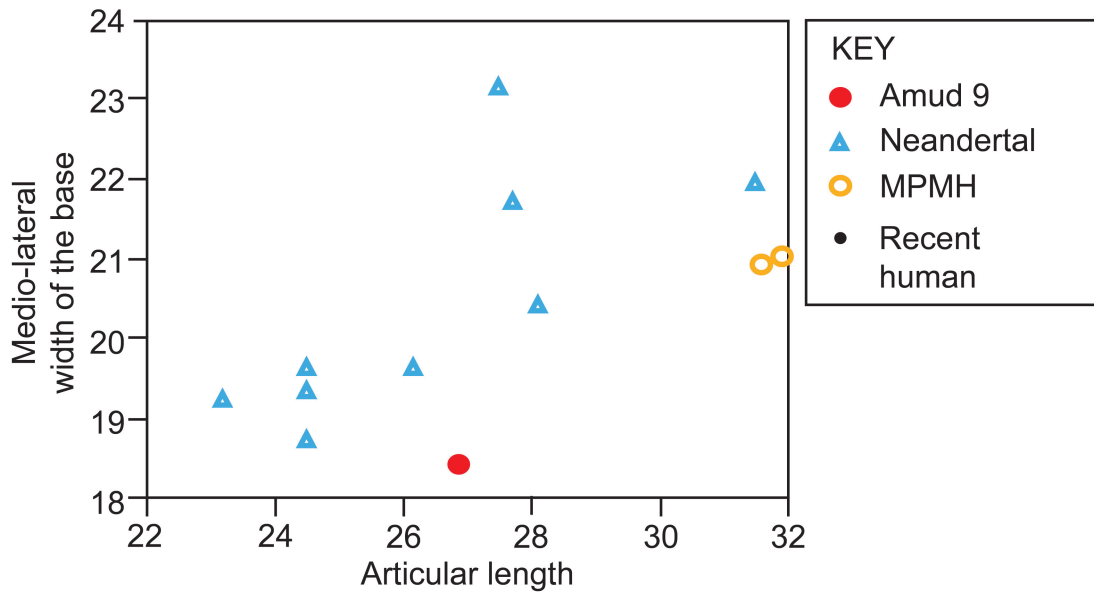


Figure 9. Articular length versus medio-lateral width of the base of proximal pedal phalanx I of Amud 9 and comparative samples. MPMH stands for Middle Paleolithic modern humans.

(EQH3) are strongly built but have a relatively small femoral distal epiphysis, although its narrow epiphyseal width may be pathological (Been et al. 2017b). The individuals from Shanidar display variation in size and massiveness and sometimes lack features considered characteristic of Western European “classic” Neandertals (Trinkaus, 1983, 1984, 1995). The hominin remains from Amud, including Amud 9, fit within this broad pattern. This pattern also characterizes the Middle Pleistocene sample of Sima de los Huesos (Arsuaga et al. 2015; Bonmatí et al. 2010; Pablos et

al. 2013a, 2014) as well as the Early Pleistocene sample of *Homo antecessor* from Atapuerca (Pablos et al. 2012) and the earlier *Homo* sp. from the TE9 level from the Sima del Elefante in Atapuerca (Lorenzo et al. 2015).

The MP Paleolithic subunits B1 – B2 at Amud, which contained most of the hominins including Amud 9, are dated near the very end of the MP material culture sequence in the southern Levant (see above). This set of dates overlaps the re-appearance of modern humans in the region, dated at Manot Cave to at least  $54.7 \pm 5.5$  ka (arithmetic mean  $\pm$  2 SD) or to  $51.8 \pm 4.5$  ka (weighted mean  $\pm$  2 SD) based on U-Th age of the calcite crust covering the Manot calvarium (Hershkovitz et al. 2015). Intriguingly, the date for the (context-devoid) Manot calvarium falls before the start of the UP at Manot (Alex et al. 2017) and other sites in the region (Bosch et al. 2015; Douka et al. 2013; Rebollo et al. 2011) that have been dated with state-of-the-art methods. The latest MP at Amud also overlaps temporally with the estimated date of an interbreeding event between modern humans and Neandertals at 50–60 ka (Fu et al. 2014; Sankararaman et al. 2012) that left a clear legacy of approximately 2% Neandertal ancestry in the genomes of populations outside of Africa. The latest MP at Shovakh Cave, located only approximately 500m up the canyon from Amud Cave, dates to  $45.5 \pm 3.7$  ka by OSL (Friesem et al. 2019), and thus occurs at the tail end of the predicted time for the major pulse of Neandertal admixture into extant Eurasian genomes.

Given this background, it is notable that Amud I, the most complete hominin from the site, has a tall stature and straight rather than bowed radius. These traits may be evidence of admixture with modern humans or, alternatively, simply reflect a larger amount of skeletal (and perhaps genetic) variation in the Near East relative to Upper Pleistocene European Neandertals. The earlier hominins from

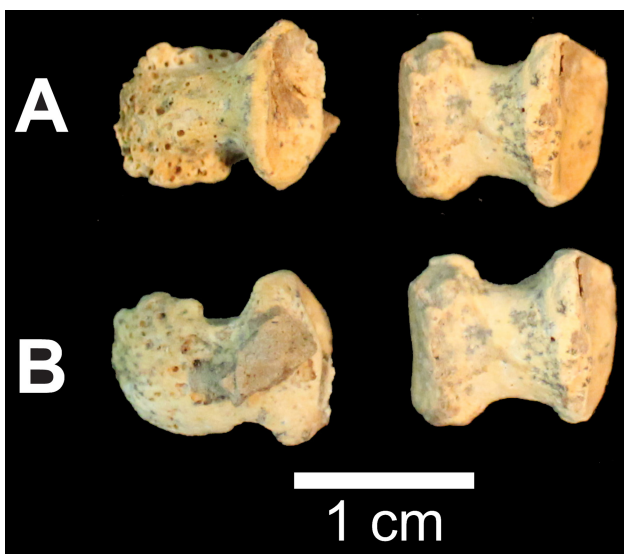


Figure 10. Intermedial and distal pedal phalanges of digit II-IV of Amud 9: A) superior view of distal (left) and intermediate (right) phalanges; B) inferior views of distal (left) and intermediate (right) phalanges.

TABLE 9. MEASUREMENTS OF THE INTERMEDIATE PEDAL PHALANX (IPP) II-IV.

	Amud 9	Tabun C1 <sup>b</sup>	Amud I	Neandertals <sup>c</sup>	Skhul IV <sup>b</sup>	Neandertals <sup>d</sup>	Skhul IV <sup>b</sup>	Neandertals <sup>e</sup>	Skhul IV
		MPP II (R)	MPP II	MPP II	II (L)	MPP III	III (L)	MPP IV	IV (L)
<b>Maximum length</b>	11.6	--	17.0	--	--	--	--	--	
<b>Articular length</b>	10.5	10.2	14.6	12.3±1.5	16	12.0±1.3	15.5	11.4±1.9	14.2
<b>Width of the base (medio-lateral)</b>	9.9	9.7	12.5	10.6±1.3	12	10.8±1.6	11	10.8±1.6	9.5
<b>Height of the base (dorso-plantar)</b>	8.4	--	10.5 <sup>a</sup>	9.2±1.0	9.6	8.8±0.6	9.5	9.2±1.3	6
<b>Width of distal articular surface</b>	14.5	9.3	11.5	9.7±1.0	9.8	9.1±2.6	9.3	8.7±2.4	9.3
<b>Midshaft medio-lateral breadth</b>	6.8	6.6	8.6	7.7±1.3	8.6	7.8±1.3	8.0	7.4±1.8	8
<b>Midshaft dorso-plantar height</b>	--	4.2	5.3	4.6±0.5	7.2	4.8±0.5	6.0	4.7±0.6	6

<sup>a</sup>Includes a slight exostosis on dorsal surface that adds approximately 1mm.

<sup>b</sup>Data from Trinkaus (1975a).

<sup>c</sup>Data from Trinkaus (1975a); sample comprises Amud I (R), La Ferrassie 1 (R), La Ferrassie 2 (R), Kiik-Koba 1 (R), Krapina a (254.5) (R), Tabun C1 (R), Shanidar 4 (L).

<sup>d</sup>Data from Trinkaus (1975a); sample includes La Ferrassie 1 (R), La Ferrassie 2 (R), Kiik-Koba 1 (R), Krapina c (254.3) (L), Shanidar 4 (R).

<sup>e</sup>Data from Trinkaus (1975a); sample comprises La Ferrassie 1 (L), La Ferrassie 2 (R), Kiik-Koba 1 (R), Krapina f (254.6) (R), Shanidar 4 (R).

Sima de los Huesos are both taller, on average, than Upper Pleistocene European Neandertals (Carretero et al. 2012) and show a substantial range of radial bowing (Arsuaga et al. 2015). Thus, the morphology of Amud I may also be consistent with no admixture with modern humans or, at most, only a small amount. If Amud I is not intermediate in morphology between earlier Neandertals in the Near East and modern humans, this might imply a relatively sudden appearance of a substantial morphological difference between Neandertals and the later modern humans in the eastern Mediterranean. Fossils of the postcranial remains of the earliest modern humans that post-date Neandertals in the Levant are needed to test this hypothesis.

Another caveat must be added. There is a notable amount of morphological similarity in some aspects of the pedal remains of Neandertals and the MP modern humans from Skhul and Qafzeh, as is reflected in the results of the discriminant analyses of Amud 9's talus and first metatar-

sal. It is possible that this similarity reflects admixture, a hypothesis that finds at least some support from ancient DNA (Kuhlwilm et al. 2016; Lorente-Galdos et al. 2019; Posth et al. 2017). Furthermore, the extent to which functional demands at the ankle, including from postural habits like squatting, may affect the morphology of the talus and thus influence morphological similarities remains largely unknown. However, a recent structured analysis by Sorrentino et al. (2020a), designed to tease apart the influences of terrain, footwear, and mode of subsistence, found that the tali of recent, highly mobile hunter-gatherers who went barefoot or wore minimal footwear had a relatively short and thick talar neck, a medially deflected head and neck, and a more laterally projecting articular facet for the fibular malleolus. These features generally accord with some of the differences between MP and modern hominins and suggest that similarities in unshod locomotion may drive some of the similarities in talar shape between MP mod-

TABLE 10. MEASUREMENTS OF THE DISTAL PEDAL PHALANX II-IV.

	Amud 9	Tabun C1	Neandertals <sup>a</sup>	Skhul IV <sup>b</sup>	Neandertals <sup>c</sup>	Skhul IV <sup>b</sup>	Neandertals <sup>c</sup>
Ray	?	II (R)	II (n=6)	II (R)	III (n=2)	III (R)	IV (n=2)
Maximum length	14.2	--	--	--	--	--	--
Articular length	12.0	11.7	11.3±0.5	11.0	12.0	10.5	10.5
Width of the base	9.8	9.6	11.1±1.6	13.0	11.1	10.0	8.8
Dorso-plantar height of the base	7.3	7.3	8.3±1.5	6.0	7.7	7.0	8.2
Midshaft height (dorso-plantar)	--	5.4	6.2±1.0	--	6.2	6.0	6.0
Midshaft breadth	6.0	--	6.7±1.0	--	6.4	5.5	6.8
Width of the apical tuft	8.2	--	10.0±1.6	--	9.6	7.0	9.6

Length of apical tuft for Amud 9: 6.4mm.

<sup>a</sup>Data from Trinkaus (1975a, 1983); sample comprises Kiik-Koba 1 (cast, R), Krapina a (254.2) (R), Tabun C1 (R), Shanidar 4 (side indeterminate), La Ferrassie 1 (ray II or III, side indeterminate), and Amud I (66) (ray II or III, side indeterminate).

<sup>b</sup>Data from Trinkaus (1975a).

<sup>c</sup>Data from Trinkaus (1975a, 1983); sample comprises Shanidar 4 (probably ray III, R), and Kiik-Koba 1 (cast, R).

ern humans and Neandertals. Some of these aspects of talar shape, especially the orientations of curved articular surfaces are captured best by geometric morphometric approaches (DeSilva et al. 2018; Rosas et al. 2017; Sorrentino et al. 2020a, 2020b)

Since our submission of this paper, Borgel et al. (in press) have published an analysis of a partial left foot from the Aurignacian-bearing deposits of Manot Cave in Israel. The foot includes a talus (MC-14) and first metatarsal (MC-18) that can be compared to Amud 9. The Manot foot belonged to a small individual with a talar length (M1) of 44.8mm (vs. 48.2mm in Amud 9) and a length (M1) of the first metatarsal of 65.1mm (vs. 57.2mm in Amud 9) (Borgel et al. 2019). Interestingly, the Manot talus has a short neck, which might align the specimen with Neandertals, but this morphology turns out to be a shared trait of nearly all *Homo* fossils, including non-recent modern humans and especially by MPMH (Pablos et al. 2012, 2013b; Pearson et al. 2008). MC-14 also has an only moderately projecting facet for the lateral malleolus, which would be unusual for a Neandertal. The Manot first metatarsal has a narrow midshaft width (12.4mm vs. 14.1mm in Amud 9) in pro-

portion to its length, which would push it towards modern humans. We ran discriminant analyses on a reduced set of measurements shared by our data set and the Manot talus and first metatarsal; the first metatarsal emerged as clearly modern while the talus sat in the zone of overlap between UP, MPMH, and Neandertal tali (results not shown). Borgel et al. (in press) concluded that, on the whole, the Manot foot was a modern human; we concur.

The archaeological record of the late MP at Amud Cave provides no impression of a population in crisis (see also Ekshtain et al. 2019 for a similar conclusion based on archaeological analysis of the 'Ein Qashish site). It is more likely that one must look to extrinsic factors to understand the demise of the MP cultural phenomenon and the end of the Neandertals in the eastern Mediterranean. One recent suggestion is that Late MP was a period of increased interactions within the Near East and beyond, precipitating a series of innovations including emerging UP technologies (Goring-Morris and Belfer-Cohen 2020; Greenbaum et al. 2019a). An intriguing hypothesis by Greenbaum et al. (2019b) proposes that diseases introduced by both populations to each other when they met may have been the driv-

ing factor in the dynamics of the contact zone and that the flow of alleles conveying resistance or immunity to these diseases gradually eliminated the boundary between the species. Greenbaum et al. (2019b) speculate that the package of pathogens introduced by modern humans may have had a more severe effect on Neandertals than the set of pathogens that modern humans acquired from Neandertals or the new, Eurasian environment had on modern humans. Whatever the case, the biological consequences for Levantine Neandertals appear to have been ultimately catastrophic, leading to the disappearance of their phenotype and dominance in most of the genome of the survivors of genes inherited from African modern humans.

## CONCLUSIONS

Amud 9, a partial right foot of a hominin from the late MP of Amud Cave, Israel, was recovered in 1993 and briefly discussed and pictured by Hovers et al. (1995). The foot consists of a crushed distal tibia, an almost complete talus, a first metatarsal, proximal pedal phalanx I, one pedal intermediate phalanx (most likely of ray II, but possibly of III or IV), and a distal pedal phalanx of ray II-IV (but most likely II or III). Initially the foot also preserved the distal fibula and another metatarsal (probably II), but these disintegrated into small fragments and can no longer be evaluated. Based on the field photographs, the lost elements appear to have been strikingly similar in size to homologous elements of Tabun C1, and it is most probable that Amud 9 was also a female Neandertal.

The tibia is crushed superiorly, the talar articular surface and medial malleolus are preserved. Much more can be said of the talus, which is most like tali of Neandertals, Middle Pleistocene modern humans, and Sima de los Huesos. The similarity to Sima de los Huesos in the CVA on raw data is largely due to the relatively wide posterior portion of the trochlea. This special point of similarity to Sima de los Huesos disappears in the CVA on shape data, which finds Neandertals and Middle Paleolithic moderns to be the most similar to Amud 9. The talus of Amud 9 has a short head and neck relative to the length of the trochlea and a markedly projecting facet for the lateral (fibular) malleolus. These features also resemble Neandertals as well as the tali of the early modern humans from Qafzeh and Skhul (Rhoads and Trinkaus 1977) but differ from the morphology common in more recent humans.

The first metatarsal is also fairly well preserved. It falls with Neandertals in discriminant space, although metatarsals from Skhul and Qafzeh also resemble it, and it differs from more recent humans. Its relatively high proximal end, proximo-distally short length, and comparatively wide diaphysis and head drive these patterns of resemblance. The proximal pedal phalanx I is relatively long compared to most Neandertals. The intermediate pedal phalanx as well as the distal pedal phalanx are short and relatively broad, like those of Neandertals.

Amud 9's stature was estimated to be 160.6±2.8 cm (from metatarsal I), 163.4±4.67 cm (from the talus), or 159.7±2.6 (from both). Amud 9's body mass was estimated

to have been 59.9kg -7.7/+8.9kg. This indicates a slightly slimmer physique than those of the means for Eskimo and Aleut females assembled by Ruff (1994), and parallels the relatively slim physique that Endo and Kimura (1970) reconstructed for Amud I.

On the whole, Amud 9 fits among the morphologically diverse group of Near Eastern Neandertals. Although a relatively substantial admixture with earlier modern humans in the Near East cannot be ruled out given the presence of overlapping features in their feet as well as other portions of the skeleton (Arensburg and Belfer-Cohen 1998), the morphology of the distal leg and foot bones provides little if any indication of admixture with modern humans that led to the genetic swamping—and replacement—of Neandertals in the Levant within a few thousand years after Amud 9 lived.

## ACKNOWLEDGEMENTS

Excavations at Amud Cave were made possible by grants from the L.S.B. Leakey Foundation, the Irene Levi-Sala Care Foundation, the Institute of Human Origins, the Jerusalem Center for Anthropological Research, and the Institute of Archaeology, Hebrew University. We are grateful to all of these institutions for support and to the many volunteers who helped to excavate the site and process the resulting materials in the laboratory. The availability of the comparative collection, both modern and fossil, would have not been possible without the help and collaboration of multiple institutions and the people that allowed us access to important collections under their care and who kindly provided assistance. Thanks to E. Trinkaus and C. Lorenzo for kindly providing some comparative data. Comments by Zach Throckmorton and an anonymous reviewer helped to improve the paper. Part of this research was supported by the Spanish MCI project PGC2018-093925-B-C33 and PGC2018-093925-B-C31 (MCI/AEI/FEDER, UE). We dedicate this paper to the memory of Ofer Bar-Yosef (1937–2020).

## ENDNOTES

<sup>1</sup>One of us (Rak) considers there to be no evidence in the fossils of admixture between Neandertals and modern humans.

## REFERENCES

- Abadi, I., Bar-Yosef, O., and Belfer-Cohen, A. (2020). Kebara V – A contribution to the study of the Middle-Upper Paleolithic transition. *PaleoAnthropology* 2020, 1–28.
- Alex, B., Barzilai, O., Hershkovitz, I., Marder, O., Berna, F., Caracuta, V., Abulafia, T., Davis, L., Goder-Goldberger, M., Lavi, R., Mintz, E., Regev, L., Bar-Yosef Mayer, D., Tejero, J.-M., Yeshurun, R., Ayalon, A., Bar-Matthews, M., Yasur, G., Frumkin, A., Latimer, B., Hans, M. G., and Boaretto, E. 2017. Radiocarbon chronology of Manot Cave, Israel and Upper Paleolithic dispersals. *Science Advances* 3, e1701450.
- Alperson-Afil, N. and Hovers, E. 2005. Differential use of space at the Neandertal site of Amud Cave, Israel. *Eurasian Prehistory* 3, 3–22.
- Alonso-Llamazares, C. and Pablos, A. 2019. Sex estima-

- tion from the calcaneus and talus using discriminant function analysis and its possible application in fossil remains. *Archaeological and Anthropological Sciences* 11, 4927–4946
- Arensburg, B. 1991. The vertebral column, thoracic cage and hyoid bone. In *Le squelette moustérien de Kébara 2*, Bar-Yosef, O. and Vandermeersch, B. (eds.). Éditions du CNRS, Paris, pp. 113–146.
- Arensburg, B. and Belfer-Cohen, A. 1998. *Sapiens* and Neandertals: rethinking the Levantine Middle Paleolithic transition. In *Neandertals and Modern Humans in Western Asia*, Akazawa, T., Aoki, K., and Bar-Yosef, O. (eds.). Plenum, New York, pp. 311–322.
- Arsuaga, J.L., Lorenzo, C., Carretero, J.-M., Gracia, A., Martínez, I., García, N., Bermúdez de Castro, J.-M., and Carbonell, E. 1999. A complete human pelvis from the Middle Pleistocene of Spain. *Nature* 399, 255–258.
- Arsuaga, J.L., Martínez, I., Arnold, L.J., Aranburu, A., Gracia-Téllez, A., Sharp, W.D., Quam, R.M., Falguères, C., Pantoja-Pérez, A., Bischoff, J., Poza-Rey, E., Parés, J.M., Carretero, J.M., Demuro, M., Lorenzo, C., Sala, N., Martínón-Torres, M., García, N., Alcázar de Velasco, A., Cuenca-Bescós, G., Gómez-Olivencia, A., Moreno, D., Pablos, A., Shen, C.-C., Rodríguez, L., Ortega, A.I., García, R., Bonmatí, A., Bermúdez de Castro, J.M., and Carbonell, E., 2014. Neandertal roots: cranial and chronological evidence from Sima de los Huesos. *Science* 344, 1358–1363.
- Arsuaga, J. L., Carretero, J.-M., Lorenzo, C., Gómez-Olivencia, A., Pablos, A., Rodríguez, L., García-González, R., Bonmatí, A., Quam, R. M., Pantoja-Pérez, A., Martínez, I., Aranburu, A., Gracia-Téllez, A., Poza-Rey, E., Sala, N., García, N., Alcázar de Velasco, A., Cuenca Bescós, G., Bermúdez de Castro, J.M., and Carbonell, E. 2015. Postcranial morphology of the Middle Pleistocene humans from Sima de los Huesos, Spain. *Proceedings of the National Academy of Sciences USA* 112, 11524–11529.
- Bailey, S., Hublin, J.-J. and Weaver, T. D. 2017. The dentition of the earliest modern humans: how ‘modern’ are they? In *Human Paleontology and Prehistory: Contributions in Honor of Yoel Rak*, Marom, A. and Hovers, E. (eds.). Springer, New York, pp. 215–232.
- Been, E., Peleg, S., Marom, A., and Barash, A. 2010. Morphology and function of the lumbar spine of the Kebara 2 Neandertal. *American Journal of Physical Anthropology* 142, 549–557.
- Been, E., Gómez-Olivencia, A., Kramer, P. A., and Barash, A. 2017a. 3D Reconstruction of spinal posture of the Kebara 2 Neanderthal. In *Human Paleontology and Prehistory: Contributions in Honor of Yoel Rak*, Marom, A. and Hovers, E. (eds.). Springer, New York, pp. 239–251.
- Been, E. Hovers, E., Ekshtain, R., Malinski-Buller, A., Agha, N., Barash, A., Mayer, D. E. B.-Y., Benazzi, S., Hublin, J.-J., Levin, L., Greenbaum, N., Mitki, N., Oxilla, G., Porat, N., Roskin, J., Soudack, M., Yeshurun, R., Shachack-Gross, R., Nir, N., Stahlschmidt, M. C., Rak, Y., and Barzilai, O. 2017b. The first Neanderthal remains from an open-air Middle Palaeolithic site in the Levant. *Scientific Reports* 7, 2958.
- Bar-Yosef, O. 2000. The Middle and Early Upper Paleolithic in Southwest Asia and neighboring regions. In *The Geography of Neandertals and Modern Humans in Europe and the Greater Mediterranean (Peabody Museum Bulletin 8)*, Bar-Yosef, O. and Pilbeam, D. (eds.). Peabody Museum of Archaeology and Ethnology, Harvard University, Cambridge, MA, pp. 107–156.
- Bar-Yosef, O. and Vandermeersch, B. 1981. Notes concerning the possible age of the Mousterian layers in Qafzeh Cave. In *Préhistoire du Levant: chronologie et organisation de l'espace depuis les origines jusqu'au Vie millénaire*, Cauvin, J. and Sanlaville, P. (eds.). C.N.R.S., Paris, pp. 281–286.
- Barnett, C., 1954. Squatting facets on the European talus. *Journal of Anatomy* 88, 509–513.
- Belmaker, M. and Hovers, E. 2011. Ecological change and the extinction of the Levantine Neanderthals: implications from a diachronic study of micromammals from Amud Cave, Israel. *Quaternary Science Reviews* 30, 3196–3209.
- Bonmatí, A., Gómez-Olivencia, A., Arsuaga, J.L., Carretero, J.M., Gracia, A., Martínez, I., Lorenzo, C., Bermúdez de Castro, J.M., and Carbonell, E. 2010. Middle Pleistocene lower back and pelvis from an aged human individual from the Sima de los Huesos site, Spain. *Proceedings of the National Academy of Sciences USA* 107, 18386–18391.
- Borgel, S., Latimer, B., McDermott, Y., Sarig, R., Pokhrojaev, A., Abulafia, T., Goder-Goldberger, M., Barzilai, O., and May, H. in press. Early Upper Paleolithic human foot bones from Manot Cave, Israel. *Journal of Human Evolution*. <https://doi.org/10.1016/j.jhevol.2019.102668>.
- Bosch, M.D., Mannino, M.A., Prendergast, A.L., O’Connell, T.C., Demarchi, B., Taylor, S.M., Niven, L., Van Der Plicht, J., and Hublin, J.-J. 2015. New chronology for Ksâr ‘Akil (Lebanon) supports Levantine route of modern human dispersal into Europe. *Proceedings of the National Academy of Sciences USA* 112, 7683–7689.
- Bouille, E.-L. 2001a. Osteological features associated with ankle hyperdorsiflexion. *International Journal of Osteoarchaeology* 11, 345–349.
- Bouille, E.-L. 2001b. Evolution of two human skeletal markers of the squatting position: a diachronic study from Antiquity to the Modern Age. *American Journal of Physical Anthropology* 115, 50–56.
- Bräuer, G. 1988. Osteometrie. In *Anthropologie*, Knussman, R. (ed.). Gustav Fischer Verlag, Stuttgart, pp. 160–231.
- Carretero, J.-M., Rodríguez, L., García-González, R., Arsuaga, J. L., Gómez-Olivencia, A., Lorenzo, C., Bonmatí, A., Gracia, A., Martínez, I., and Quam, R. 2012. Stature estimation from complete long bones in the Middle Pleistocene humans from the Sima de los Huesos, Sierra de Atapuerca (Spain). *Journal of Human Evolution* 62, 242–255.
- Chinzei, K. 1970. The Amud cave site and its deposits. In *The Amud Man and His Cave Site*, Suzuki, H. and Takai, F. (eds.). Academic Press of Japan, Tokyo, pp. 77–114.
- Churchill, S.E., Pearson, O.M., Grine, F.E., Trinkaus, E.,

- and Holliday, T.W. 1996. Morphological affinities of the proximal ulna from Klasies River Mouth Main Site: archaic or modern? *Journal of Human Evolution* 31, 213–237.
- Corrain, C. 1977. I resti scheletrici umani della sepoltura epigravettiana del Riparo Tagliente in Valpantena (Verona). *Bollettino del Museo Civico di Storia Naturale di Verona* 4, 35–79.
- Dalén, L., Orlando, L., Shapiro, B., Brandström-Durling, M., Quam, R., Gilbert, M. T., Díez Fernández-Lomana, J. C., Willerslev, E., Arsuaga, J. L., and Götherström, A. 2012. Partial genetic turnover in Neandertals: continuity in the East and population replacement in the West. *Molecular Biology and Evolution* 29, 1893–1897.
- Darroch, J.N. and Mosimann, J.E. 1985. Canonical and principle components of shape. *Biometrika* 72, 241–252.
- DeGiorgio, M., Jakobsson, M., and Rosenberg, N.A. 2009. Explaining worldwide patterns of human genetic variation using a coalescent-based serial founder model of migration outward from Africa. *Proceedings of the National Academy of Sciences USA* 106, 16057–16062.
- DeSilva, J., McNutt, E., Benoit, J., and Zipfel, B. 2018. One small step: a review of Plio-Pleistocene hominin foot evolution. *Yearbook of Physical Anthropology* 168 (S67), 63–140.
- Dodo, Y., Kondo, O., Muhesen, S., and Akazawa, T. 1998. Anatomy of the Neandertal infant skeleton from Dederiyeh Cave, Syria. In *Neandertals and Modern Humans in Western Asia*, Akazawa, T., Aoki, K., and Bar-Yosef, O. (eds). Plenum, New York, pp. 323–338.
- Douka, K., Bergman, C.A., Hedges, R.E.M., Wesselingh, F.P., and Higham, T.F.G. 2013. Chronology of Ksar Akil (Lebanon) and implications for the colonization of Europe by anatomically modern humans. *PloS One* 8/9, e72931.
- Ekshtain, R., Ilani, S., Segal, I., and Hovers, E. 2017. Local and nonlocal procurement of raw material in Amud Cave, Israel: the complex mobility of late Middle Paleolithic groups. *Geoarchaeology* 32, 189–214.
- Ekshtain, R. and Tryon, C.A. 2019. Lithic raw material acquisition and use by early *Homo sapiens* at Skhul, Israel. *Journal of Human Evolution* 127, 149–170.
- Endo, B. and Kimura, T. 1970. Postcranial skeleton of the Amud Man. In *The Amud Man and His Cave Site*, Suzuki, H. and Takai, F. (eds.). Academic Press of Japan, Tokyo, pp. 231–406.
- Fagundes, N.J.R., Ray, N., Beaumont, M., Neuenschwander, S., Salzano, F.M., Bonatto, S.L., and Excoffier, L. 2007. Statistical evaluation of alternative models of human evolution. *Proceedings of the National Academy of Sciences USA* 104, 17614–17619.
- Foley, R. and Lahr, M.M. 1997. Mode 3 Technologies and the evolution of modern humans. *Cambridge Archaeological Journal* 7, 3–36.
- Friesem, D. E., Malinsky-Buller, A., Ekshtain, R., Gur-Arieh, S., Vaks, A., Mercier, N., Richard, M., Guérin, G., Valladas, H., Auger, F., and Hovers, E. 2019. New data from Shovakh Cave and its implications for reconstructing Middle Paleolithic settlement patterns in the Amud drainage, Israel. *Journal of Paleolithic Archaeology*, <https://doi.org/10.1007/s41982-019>.
- Fu, Q., Mittnik, A., Johnson, P.L.F., Bos, K., Lari, M., Bolongino, R., Sun, C., Giemsch, L., Schmitz, R., Burger, J., Ronchitelli, A.M., Martini, F., Cremonesi, R.G., Svoboda, J., Bauer, P., Caramelli, D., Castellano, S., Reich, D., Pääbo, S., and Krause, J. 2013. A revised timescale for human evolution based on ancient mitochondrial genomes. *Current Biology* 23, 553–559.
- Fu, Q., Li, H., Moorjani, P., Jay, F., Slepchenko, S.M., Bondarev, A.A., Johnson, P.L.F., Aximu-Petri, A., Prufer, K., de Filippo, C., Meyer, M., Zwyns, N., Salazar-García, D.C., Kuzmin, Y.V., Keates, S.G., Kosintsev, P.A., Razhev, D.I., Richards, M.P., Peristov, N.V., Lachmann, M., Douka, K., Higham, T.F.G., Slatkin, M., Hublin, J.-J., Reich, D., Kelso, J., Viola, T.B., Pääbo, S. 2014. Genome sequence of a 45,000-year-old modern human from western Siberia. *Nature* 514, 445–449.
- Gambier, D. 1981. *Étude de l'astragale chez les Neandertaliens*. Ph.D. Dissertation. Paris, Université Pierre et Marie Curie.
- Gómez-Olivencia, A., Eaves-Johnson K.L., Franciscus, R.G., Carretero, J.M., AND Arsuaga, J.M. 2009. Kebara 2: new insights regarding the most complete Neandertal thorax. *Journal of Human Evolution* 57, 75–90.
- Gómez-Olivencia, A., Barash, A., García-Martínez, D., Arlegi, M., Kramer, P., Bastir, M., and Been, E., 2018. 3D virtual reconstruction of the Kebara 2 Neandertal thorax. *Nature Communications* 9, 4387.
- Goring-Morris, N. and Belfer-Cohen, A. 2020. Noisy beginnings: The Initial Upper Palaeolithic in Southwest Asia. *Quaternary International*. <https://doi.org/10.1016/j.quaint.2020.01.017>.
- Greenbaum, G., Friesem, D.E., Hovers, E., Feldman, M.W., and Kolodny, O. 2019a. Was inter-population connectivity of Neanderthals and modern humans the driver of the Upper Paleolithic transition rather than its product? *Quaternary Science Reviews* 217, 316–329.
- Greenbaum, G., Getz, W.M., Rosenberg, N.A., Feldman, M.W., Hovers, E., and Kolodny, O. 2019b. Disease transmission and introgression can explain the long-lasting contact zone of modern humans and Neanderthals. *Nature Communications* 10, 5003. <https://doi.org/10.1038/s41467-12862-7>.
- Hallin, K.A., Schoeninger, M.J., and Schwarcz, H.P. 2012. Paleoclimate during Neandertal and anatomically modern human occupation at Amud and Qafzeh, Israel: the stable isotope data. *Journal of Human Evolution* 62, 59–73.
- Hershkovitz, I., Marder, O., Ayalon, A., Bar-Matthews, M., Yasur, G., Boaretto, E., Caracuta, V., Alex, B., Frumkin, A., Goder-Goldberger, M., Gunz, P., Holloway, R., Latimer, B., Lavi, R., Matthews, A., Slon, V., Bar-Yosef Mayer, D., Berna, F., Bar-Oz, G., Yeshurun, R., May, H., Hans, M. G., Weber, G., and Barzilai, O. 2015. Levantine cranium from Manot Cave (Israel) foreshadows the first European modern humans. *Nature* 520, 216–219.

- Hartman, G., Hovers, E., Hublin, J.-J., and Richards, M. 2015. Isotopic evidence for Last Glacial climatic impacts on Neanderthal gazelle hunting territories at Amud Cave, Israel. *Journal of Human Evolution* 84, 71–82.
- Henn, B.M., Cavalli-Sforza, L.L., and Feldman, M.W. 2012. The great human expansion. *Proceedings of the National Academy of Sciences USA* 109, 17758–17764.
- Hovers, E. 1998. The lithic assemblages of Amud Cave, In *Neandertals and Modern Humans in Western Asia*, T. Akazawa, T. Aoki, K. and Bar-Yosef, O. (eds.). Plenum, New York, pp. 143–163.
- Hovers, E. 2004. Cultural ecology at the Neanderthal site of Amud Cave, Israel. In *Arkheologiya i Paleoekologiya Evrasii [Archaeology and Paleoecology of Eurasia]. Papers in Honor of Vadim Ranov*, Derevianko, A.P., and Nokhrina, T.I. (eds.). Institute of Archaeology and Ethnography SB RAS Press, Novosibirsk, pp. 218–231.
- Hovers, E. 2007. The many faces of cores-on-flakes: a perspective from the Levantine Mousterian. In *Cores or Tools? Alternative Approaches to Stone Tool Analysis*, McPherron, S.P. (ed.). Cambridge Scholars Press, Cambridge, pp. 42–74.
- Hovers, E. and Belfer-Cohen, A. 2013. On variability and complexity: lessons from the Levantine Middle Paleolithic record. *Current Anthropology* 54, S337–S357.
- Hovers, E., Rak, Y., and Kimbel, W.H. 1991. Amud Cave - the 1991 season. *Journal of the Israel Prehistoric Society* 24, 152–157.
- Hovers, E., Rak, Y., Lavi, R., and Kimbel, W.H. 1995. Hominid remains from Amud Cave in the context of the Levantine Middle Paleolithic. *Paléorient* 21, 47–61.
- Hovers, E., Kimbel, W.H., and Rak, R. 2000. The Amud 7 skeleton--still a burial. Response to Gargett. *Journal of Human Evolution* 39, 253–260.
- Hovers, E., Malinsky-Buller, A., Goder-Goldberger, M., and Ekshtain, R. 2011. Capturing a moment: identifying short-lived activity locations at Amud Cave, Israel. In *The Lower and Middle Paleolithic in the Middle East and Neighboring Regions (ERAUL 126)*, Le Tensorer, J.-M., Jagher, R. and Otte, M. (eds.). Presses Universitaires de Liège, Liège, pp. 101–114.
- Hovers, E., Ullman, M., and Rak, Y. 2017. Palaeolithic occupations in Nahal Amud. In *Quaternary of the Levant: Environments, Climate, and Humans*, Enzel, Y. and Bar-Yosef, O. (eds.). Cambridge University Press, Cambridge, pp. 255–266.
- Howell, F.C. 1957. The evolutionary significance of variation and varieties of “Neanderthal” man. *Quarterly Review of Biology* 32, 330–347.
- Howell, F.C. 1958. Upper Pleistocene men of the Southwest Asian Mousterian. In *Hundert Jahre Neanderthaler*, von Koenigswald, G.H.R. (ed.). Kemink en Zoon, Utrecht, pp. 185–198.
- Hublin, J.-J. 2015. The modern human colonization of western Eurasia: when and where? *Quaternary Science Reviews* 118, 194–210.
- Inbar, M. and Hovers, E. 1999. The morphological development of the Lower Amud River in the Upper Pleistocene. *Horizons in Geography* 50, 27–38 (in Hebrew).
- Kolska Horwitz, L. and Hongo, H. 2008. Putting meat back on old bones: a reassessment of Middle Palaeolithic fauna from Amud Cave (Israel). In *Archaeozoology of the Near East. VIII. Tome I*, Vila, E., Gourichon, L., Choyke, A.M., and Buitenhuis, H. (eds.). Maison de l’Orient et de la Méditerranée, Lyon, pp. 45–64.
- Kondo, O. and Dodo, Y. 2002. The postcranial bones of the Neanderthal child burial no. 1. In *Neanderthal Burials: Excavations of the Dederiyeh Cave, Afrin, Syria. Studies in Honor of Hisashi Suzuki*, Akazawa, T. and Muhesen, S. (eds.). International Research Center for Japanese Studies, Kyoto, pp. 139–214.
- Kondo, O. and Ishida, H. 2002. The postcranial bones of the Neanderthal child of burial no. 2. In *Neanderthal Burials: Excavations of the Dederiyeh Cave, Afrin, Syria. Studies in Honor of Hisashi Suzuki*, Akazawa, T. and Muhesen, S. (eds.). International Research Center for Japanese Studies, Kyoto, pp. 299–321.
- Krakovsky, M. 2017. *Technological Traditions at the End of the Middle Palaeolithic in the Southern Levant? Point Reduction Sequences from Amud and Kebara Caves as a Case Study*. M.A. thesis, Jerusalem, The Hebrew University of Jerusalem.
- Kuhlwilms, M., Gronau, I., Hubisz, M. J., de Filippo, C., Prado-Martinez, J., Kircher, M., Fu, Q., Burbano, H. A., Lalueza-Fox, C., de la Rasilla, M., Rosas, A., Rudan, P., Brajkovic, D., Kucan, Ž., Gušić, I., Marques-Bonet, T., Andrés, A.M., Viola, B., Pääbo, S., Meyer, M., Siepel, A., and Castellano, S. 2016. Ancient gene flow from modern humans into eastern Neanderthals. *Nature* 530, 429–429.
- Kuhn, S.L. and Zwyns, N. 2014. Rethinking the Initial Upper Paleolithic. *Quaternary International* 347, 29–38.
- Lavi, R. 1994. *The Amud I Skull: Taxonomic Assessment and Phylogenetic Status*. M.A. thesis, Department of Anatomy and Anthropology, Tel-Aviv, Tel-Aviv University (in Hebrew).
- Li, H. and Durbin, R. 2011. Inference of human population history from individual whole-genome sequences. *Nature* 475, 493–496.
- Lorente-Galdos, B., Serra-Vidal, G., Santpere, G., Kuderna, L.K.F., Arauna, L.R., Fadhlaoui-Zid, K., Pimenoff, V.N., Soodyall, H., Zalloua, P., Marques-Bonet, T., and Comas, D. 2019. Whole-genome sequence analysis of a pan African set of samples reveals archaic gene flow from an extinct basal population of modern humans into sub-Saharan populations. *Genome Biology* 20, 77.
- Lorenzo, C., Pablos, A., Carretero, J.M., Huguet, R., Vallverdú, J., Martínón-Torres, M., Arsuaga, J.L., Carbonell, E., and Bermúdez de Castro, J.M., 2015. Early Pleistocene human hand phalanx from the Sima del Elefante (TE) cave site in Sierra de Atapuerca (Spain). *Journal of Human Evolution* 78, 114–121.
- Madella, M. Jones, M.K., Goldberg, P., Goren, Y., and Hovers, E. 2002. The exploitation of plant resources by Neanderthals in Amud Cave (Israel): the evidence from phytolith studies. *Journal of Archaeological Science* 29,

- 703–719.
- Mallick, S., Li, H., Lipson, M., Mathieson, I., Gymrek, M., Racimo, F., Zhao, M., Chennagiri, N., Nordenfelt, S., Tandon, A., Skoglund, P., Lazaridis, I., Sankararaman, S., Fu, Q., Rohland, N., Renaud, G., Erlich, Y., Willems, T., Gallo, C., Spence, J.P., Song, Y. S., Poletti, G., Baloux, F., van Driem, G., de Knijff, P., Gallego Romero, I., Jha, A.R., Behar, D.M., Bravi, C. M., Capelli, C., Hervig, T., Moreno-Estrada, A., Posukh, O.L., Balanovska, E., Balanovsky, O., Karachanak-Yankova, S., Sahakyan, H., Toncheva, D., Yepiskoposyan, L., Tyler-Smith, C., Xue, Y., Abdullah, M. S., Ruiz-Linares, A., Beall, C.M., Di Rienzo, A., Jeong, C., Starikovskaya, E.B., Metspalu, E., Parik, J., Villems, R., Henn, B.M., Hodoglugil, U., Mahley, R., Sajantila, A., Stamatoyannopoulos, G., Wee, J.T.S., Khusainova, R., Khusnutdinova, E., Litvinov, S., Ayodo, G., Comas, D., Hammer, M.F., Kivisild, T., Klitz, W., Winkler, C.A., Labuda, D., Bamshad, M., Jorde, L.B., Tishkoff, S.A., Watkins, W.S., Metspalu, M., Dryomov, S., Sukernik, R., Singh, L., Thangaraj, K., Pääbo, S., Kelso, J., Patterson, N., and Reich, D. 2016. The Simons Genome Diversity Project: 300 genomes from 142 diverse populations. *Nature* 538, 201–206.
- Matiegka, J. 1938. *Homo Předměstensis: Fosilní Člověk z Předměstí na Morave II. Ostatní Části Kostrové*. Nákaladem České Akademie Věd e Umění, Prague.
- Martin, R. and Saller, K. 1956. *Lehrbuch Der Anthropologie*. Gustav Fischer Verlag, Stuttgart.
- McCown, T.D. and Keith, A. 1939. *The Stone Age of Mount Carmel, II: The Fossil Human Remains From the Levalloiso-Mousterian*. Clarendon Press, Oxford.
- Mellars, P. 2005. The impossible coincidence. A single-species model for the origins of modern human behavior in Europe. *Evolutionary Anthropology* 14, 12–27.
- Mellars, P. 2006. Going east: new genetic and archaeological perspectives on the modern human colonization of Eurasia. *Science* 313, 796–800.
- Mercier, N., Valladas, H., Bar-Yosef, O., Vandermeersch, B., Stringer, C.B., and Joron, J.L. 1993. Thermoluminescence date for the Mousterian burial site of Es-Skhul, Mt. Carmel. *Journal of Archaeological Science* 22, 495–509.
- Meyer, M., Kircher, M., Gansauge, M.-T., Li, H., Racimo, F., Mallick, S., Schraiber, Joshua G., Jay, F., Prüfer, K., de Filippo, C., Sudmant, P.H., Alkan, C., Fu, Q., Do, R., Rohland, N., Tandon, A., Siebauer, M., Green, R.E., Bryc, K., Briggs, A.W., Stenzel, U., Dabney, J., Shendure, J., Kitzman, J., Hammer, M.F., Shunkov, M.V., Derevianko, A.P., Patterson, N., Andrés, A.M., Eichler, E.E., Slatkin, M., Reich, D., Kelso, J., and Pääbo, S. 2012. A high-coverage genome sequence from an archaic Denisovan individual. *Science* 338, 222–226.
- Mosimann, J.E. 1970. Size allometry: size and shape variables with characteristics of the log normal and generalized gamma distributions. *Journal of the American Statistical Association* 65, 930–945.
- Ohnuma, K. 1992. The significance of layer B (square 8-19) of the Amud Cave (Israel) in the Levantine Levalloiso-Mousterian: a technological study. In *The Evolution and Dispersal of Modern Humans in Asia*, Akazawa, T., Aoki, K., and Kimura, T. (eds.). Hokusen-Sha Publishing, Tokyo, pp. 83–106.
- Pablos, A., Lorenzo, C., Martínez, I., Bermúdez de Castro, J.-M., Martínón-Torres, M., Carbonell, E., and Arsuaga, J.-L., 2012. New foot remains from the Gran Dolina-TD6 Early Pleistocene site (Sierra de Atapuerca, Burgos, Spain). *Journal of Human Evolution* 63, 610–623.
- Pablos, A., Martínez, I., Lorenzo, C., Gracia, A., Sala, N., and Arsuaga, J.L. 2013a. Human talus bones from the Middle Pleistocene site of Sima de los Huesos (Sierra de Atapuerca, Burgos, Spain). *Journal of Human Evolution* 65, 79–92.
- Pablos, A., Gómez-Olivencia, A., García-Pérez, A., Martínez, I., Lorenzo, C., and Arsuaga, J.-L. 2013b. From toe to head: use of robust regression methods in stature estimation based on foot remains. *Forensic Science International* 226, 299.e1–299.e7.
- Pablos, A., Martínez, I., Lorenzo, C., Sala, N., Gracia-Téllez, A., and Arsuaga, J.-L. 2014. Human calcanei from the Middle Pleistocene site of Sima de los Huesos (Sierra de Atapuerca, Burgos, Spain). *Journal of Human Evolution* 76, 63–76.
- Pablos, A., Pantoja-Pérez, A., Martínez, I., Lorenzo, C. and Arsuaga, J.-L. 2017. Metric and morphological analysis of the foot in the Middle Pleistocene sample of Sima de los Huesos (Sierra de Atapuerca, Burgos, Spain). *Quaternary International* 433(Part A), 103–113.
- Pablos, A., Gómez-Olivencia, A., and Arsuaga, J.-L. 2019b. A Neandertal foot phalanx from the Galería de las Estatuas site (Sierra de Atapuerca, Spain). *American Journal of Physical Anthropology* 168, 222–228.
- Pablos, A., Gómez-Olivencia, A., Maureille, B., Holliday, T.W., Madelaine, S., Trinkaus, E., Couture-Veschambre, C. 2019a. Neandertal foot remains from Regourdou 1 (Montignac-sur-Vézère, Dordogne, France). *Journal of Human Evolution* 128, 17–44.
- Paoli, G., Parenti, R., and Sergi, S. 1980. Gli scheleteri mesolitici della caverna delle Arene Candide (Liguria). *Memoire dell'Instituto Italiano di Paleontologia Umana, n.s.* 3, 31–154.
- Pearson, O.M. 2000a. Activity, climate, and postcranial robusticity: implications for modern human origins and scenarios of adaptive change. *Current Anthropology* 41, 569–607.
- Pearson, O.M. 2000b. Postcranial remains and the origin of modern humans. *Evolutionary Anthropology* 9, 229–247.
- Pearson, O.M. and Busby, A.M. 2006. Physique and ecogeographic adaptations of the Last Interglacial Neandertals from Krapina. *Periodicum Biologorum* 108, 449–455.
- Pomeroy, E., Lahr, M.M., Crivellaro, F., Farr, L., Reynolds, T., Hunt, C.O., and Barker, G. 2017. Newly discovered Neandertal remains from Shanidar Cave, Iraqi Kurdistan, and their attribution to Shanidar 5. *Journal of Human Evolution* 111, 102–118.
- Posth, C., Wissing, C., Kitagawa, K., Pagani, L., van Holstein, L., Racimo, F., Wehrberger, K., Conard, N.J.,

- Kind, C.J., Bocherens, H., and Krause, J. 2017. Deeply divergent archaic mitochondrial genome provides lower time boundary for African gene flow into Neanderthals. *Nature Communications* 8, 16046.
- Prüfer, K., de Filippo, C., Grote, S., Mafessoni, F., Korlevic, P., Hajdinjak, M., Vernot, B., Skov, L., Hsieh, P., Peyrégne, S., Reher, D., Hopfe, C., Nagel, S., Maricic, T., Fu, Q., Theunert, C., Rogers, R., Skoglund, P., Chintalapati, M., Dannemann, M., Nelson, B.J., Key, F.M., Rudan, P., Kucan, Ž., Gušić, I., Golovanova, L.V., Doronichev, V.B., Patterson, N., Reich, D., Eichler, E.E., Slatkin, M., Schierup, M.H., Andrés, A.M., Kelso, J., Meyer, M., and Pääbo, S. 2017. A high-coverage Neanderthal genome from Vindija Cave in Croatia. *Science* 358, 655–658.
- Rabinovich, R. and Hovers, E. 2004. Faunal analysis from Amud Cave: preliminary results and interpretations. *International Journal of Osteoarchaeology* 14, 287–306.
- Rak, Y. 1986. The Neanderthal: a new look at an old face. *Journal of Human Evolution* 15, 151–164.
- Rak, Y. 1990. On the differences between two pelvises of Mousterian context from the Qafzeh and Kebara Caves, Israel. *American Journal of Physical Anthropology* 81, 323–332.
- Rak, Y. 1991. The pelvis. In *Le Squelette Moustérien De Kébara 2*, Bar-Yosef, O. and Vandermeersch, B. (eds.). Éditions du CNRS, Paris, pp. 147–156.
- Rak, Y. 1993. Morphological variation in *Homo neanderthalensis* and *Homo sapiens* in the Levant: a biogeographic model. In *Species, Species Concepts, and Primate Evolution*, Kimbel, W.H. and Martin, L.B. (eds.). Plenum, New York, pp. 523–536.
- Rak, Y. 1998. Does any Mousterian cave present evidence of two hominid species? In *Neanderthals and Modern Humans in Western Asia*, Akazawa, T., Aoki, K., and Bar-Yosef, O. (eds.). Plenum, New York, pp. 353–366.
- Rak, Y. and Arensburg, B. 1987. Kebara 2 Neanderthal pelvis: first look at a complete inlet. *American Journal of Physical Anthropology* 73, 227–231.
- Rak, Y., Kimbel, W.H., and Hovers, E. 1994. A Neanderthal infant from Amud Cave, Israel. *Journal of Human Evolution* 26, 313–324.
- Rak, Y., Kimbel, W.H., and Hovers, E. 1996. On Neanderthal autapomorphies discernable in Neanderthal infants: a response to Creed-Miles et al. *Journal of Human Evolution* 30, 155–158.
- Rebollo, N.R., Weiner, S., Brock, F., Meignen, L., Goldberg, P., Belfer-Cohen, A., Bar-Yosef, O., and Boaretto, E. 2011. New radiocarbon dating of the transition from the Middle to the Upper Paleolithic in Kebara Cave, Israel. *Journal of Archaeological Science* 38, 2424–2433.
- Rhoads, J.G. and Trinkaus, E. 1977. Morphometrics of the Neanderthal talus. *American Journal of Physical Anthropology* 46, 29–43.
- Rink, W.J., Schwarcz, H.P., Lee, H.K., Rees-Jones, J., Rabinovich, R., and Hovers, E. 2001. Electron spin resonance (ESR) and thermal ionization mass spectrometric (TIMS)  $^{230}\text{Th}/^{234}\text{U}$  dating of teeth in Middle Paleolithic layers at Amud Cave, Israel. *Geochronology* 16, 701–717.
- Rosas, A., Fernando, A., Bastir, M., García-Tabernero, A., Estalrich, A., Huguet, R., García-Martínez, D., Pastor, J.F., and de la Rasilla, M. 2017. Neanderthal talus bones from El Sidrón site (Asturias, Spain): a 3D geometric morphometric analysis. *American Journal of Physical Anthropology* 164, 394–415.
- Rose, J.I. and Marks, A.E. 2014. “Out of Arabia” and the Middle-Upper Palaeolithic transition in the southern Levant. *Quartär* 61, 49–85.
- Ruff, C.B. 1994. Morphological adaptation to climate in modern and fossil hominids. *Yearbook of Physical Anthropology* 37, 65–107.
- Sankararaman, S., Patterson, N., Li, H., Pääbo, S., and Reich, D. 2012. The date of interbreeding between Neanderthals and modern humans. *PLoS Genetics* 8, e1002947.
- Sankararaman, S., Mallick, S., Dannemann, M., Prüfer, K., Kelso, J., Pääbo, S., Patterson, N., and Reich, D. 2014. The genomic landscape of Neanderthal ancestry in present-day humans. *Nature* 507, 354–357.
- Sankararaman, S., Mallick, S., Patterson, D., and Reich, D. 2016. The combined landscape of Denisovan and Neanderthal ancestry in present-day humans. *Current Biology* 26, 1–7.
- Schiffels, S. and Durbin, R. 2014. Inferring human population size and separation history from multiple genome sequences. *Nature Genetics* 46, 919–925.
- Schwarcz, H.P., Grün, R., Vandermeersch, B., Bar-Yosef, O., Valladas, H., and Tchernov, E. 1988. ESR dates for the hominid burial site of Qafzeh in Israel. *Journal of Human Evolution* 17, 733–737.
- Scozzari, R., Massaia, A., D’Atanasio, E., Myres, N.M., Perego, U.A., Trombetta, B., and Cruciani, F. 2012. Molecular dissection of the basal clades in the human Y chromosome phylogenetic tree. *PloS One* 7, e49170.
- Shahack-Gross, R., Ayalon, A., Goldberg, P., Goren, Y., Ofek, B., Rabinovich, R., and Hovers, E. 2008. Formation processes of cemented features of karstic cave sites revealed using stable oxygen and carbon isotopic analysis: a case study at Middle Paleolithic Amud Cave, Israel. *Geoarchaeology* 23, 43–62.
- Shea, J. J. 2007. The boulevard of broken dreams: evolutionary discontinuity in the Late Pleistocene Levant. In *Rethinking the Human Revolution: New Behavioural and Biological Perspectives on the Origin and Dispersal of Modern Humans*, Mellars, P., Boyle, K., Bar-Yosef, O., and Stringer, C. (eds.). McDonald Institute for Archaeological Research, Cambridge, pp. 219–232.
- Shea, J.J. 2008. Transitions or turnovers? Climatically-forced extinctions of *Homo sapiens* and Neanderthals in the East Mediterranean Levant. *Quaternary Science Reviews* 27, 2253–2270.
- Simpson, S.W., Quade, J., Levin, N.E., Butler, R., Dupont-Niven, G., Everett, M., and Semaw, S. 2008. A female *Homo erectus* pelvis From Gona, Ethiopia. *Science* 322, 1089–1092.
- Soares, P., Alshamali, F., Pereira, J.B., Fernandes, V., Silva, N.M., Afonso, C., Costa, M.D., Musilová, E., Macaulay,

- V., Richards, M.B., Černý, V., and Pereira, L. 2012. The expansion of mtDNA haplogroup L3 within and out of Africa. *Molecular Biology and Evolution* 29, 915–927.
- Sorrentino, R., Stephens, N.B., Carlson, K.J., Figus, C., Fiorenza, L., Frost, S., Harcourt-Smith, W., Parr, W., Saers, J., Turley, K., Wroe, S., Belcastro, M.G., Ryan, T.M., and Benazzi, S. 2020a. The influence of mobility strategy on the human talus. *American Journal of Physical Anthropology* 171, 456–469.
- Sorrentino, R., Belcastro, M.G., Figus, C., Stephens, N.B., Turley, K., Harcourt-Smith, W., Ryan, T. M., and Benazzi, S. 2020. Exploring sexual dimorphism of the modern human talus through geometric morphometric methods. *PLoS One* 15, e0229255.
- Stringer, C.B., Grün, R., Schwarcz, H.P., and Goldberg, P. 1989. ESR dates for the hominid burial site of Es Skhul in Israel. *Nature* 338, 756–758.
- Susman, R.L., Stern, J.T., Jr., and Jungers, W.L. 1984. Arbo-reality and bipedality in the Hadar hominids. *Folia Primatologica* 43, 113–156.
- Suzuki, H. and Takai, F. (eds.) 1970. *The Amud Man and His Cave Site*. Tokyo University Press, Tokyo.
- Tillier, A.-M. 1989. The evolution of modern humans: evidence from young Mousterian individuals. In *The Human Revolution*, Mellars, P. and Stringer, C.B. (eds.). Edinburgh University Press, Edinburgh, pp. 286–297.
- Tillier, A.-M. 1998. Ontogenetic variation in Late Pleistocene *Homo sapiens* from the Near East: implications for methodological bias in reconstructing evolutionary biology. In *Neandertals and Modern Humans in Western Asia*, Akazawa, T., Aoki, K., and Ofer Bar-Yosef, O. (eds.). Plenum, New York, pp. 381–389.
- Tillier, A.-M. 1999. *Les enfants moustériens de Qafzeh: interprétation phylogénétique et paléoaurologique*. Éditions du C.N.R.S., Paris.
- Tillier, A.-M. 2005. The Tabun C1 skeleton: a Levantine Neandertal? *Journal of the Israel Prehistoric Society* 35, 439–450.
- Trinkaus, E. 1975a. *A Functional Analysis of the Neandertal Foot*. Ph.D. dissertation, University of Pennsylvania, Philadelphia.
- Trinkaus, E., 1975b. Squatting among the Neandertals: a problem in the behavioral interpretation of skeletal morphology. *Journal of Archaeological Science* 2, 327–351.
- Trinkaus, E. 1977. An inventory of the Neandertal remains from Shanidar Cave, Northern Iraq. *Sumer* 33, 9–33
- Trinkaus, E. 1983. *The Shanidar Neandertals*. Academic Press, New York.
- Trinkaus, E. 1984. Western Asia. In *The Origins of Modern Humans: A World Survey of the Fossil Evidence*, Smith, F.H. and Spencer, F. (eds.). Alan R. Liss, New York, pp. 251–293.
- Trinkaus, E. 1992. Morphological contrasts between the Near Eastern Qafzeh-Skhul and late archaic human samples: grounds for a behavioral difference? In *The Evolution and Dispersal of Modern Humans in Asia*, Akazawa, T., Aoki, K., and Kimura, T. (eds.). Hokusen-sha Publishing Co., Tokyo, pp. 277–294.
- Trinkaus, E. 1995. Near Eastern late archaic humans. *Paléorient* 21, 9–23.
- Trinkaus, E. 2015. The appendicular skeletal remains of Oberkassel 1 and 2. In *The Late Glacial Burial from Oberkassel Revisited*, Giemsch, L. and Schmitz, R.W. (eds.). Verlag Philipp von Zabern, Darmstadt, pp. 75–132.
- Trinkaus, E. and Hilton, C.E. 1996. Neandertal pedal proximal phalanges: diaphyseal loading patterns. *Journal of Human Evolution* 30, 399–425.
- Trinkaus, E. and Holliday, T. 2000. The human remains from Paviland Cave. In *Paviland Cave and the 'Red Lady': A Definitive Report*, Aldhouse-Green, S.H.R. (ed.). Western Academic and Specialist Press, Bristol, pp. 141–204.
- Trinkaus, E. and Shang, H. 2008. Anatomical evidence for the antiquity of human footwear: Tianyuan and Sung-hir. *Journal of Archaeological Science* 35, 1928–1933.
- Trinkaus, E., Buzhilova, A.P., Mednikova, M.B., and Dobrovolskaya, M.V. 2014. *The People of Sung-hir: Burials, Bodies, and Behavior in the Earlier Upper Paleolithic*. Oxford University Press, New York.
- Valladas, H., Joron, J.-L., Valladas, G., Arensburg, B., Bar-Yosef, O., Belfer-Cohen, A., Goldberg, P., H. Laville, H., Meignen, L., Rak, Y., Tchernov, E., Tillier, A.M., and Vandermeersch, B. 1987. Thermoluminescence dates for the Neandertal site at Kebara in Israel. *Nature* 330, 159–160.
- Valladas, H., Reyss, L., Joron, J.-L., Valladas, G., Bar-Yosef, O., and Vandermeersch, B. 1988. Thermoluminescence dating of Mousterian 'Proto-Cro-magnon' remains from Israel and the origin of modern man. *Nature* 331, 614–615.
- Valladas, H., Mercier, N., Joron, J.-L., and Reyss, J.-L. 1998. Gif Laboratory dates for Middle Paleolithic Levant. In *Neandertals and Modern Humans in Western Asia*, Akazawa, T., Aoki, K., and Bar-Yosef, O. (eds.). Plenum, New York, pp. 69–75.
- Valladas, H., Mercier, N., Froget, L., Hovers, E., Joron, J.-L., Kimbel, W.H., and Rak, Y. 1999. TL dates for the Neandertal site of the Amud Cave, Israel. *Journal of Archaeological Science* 26, 259–268.
- Vandermeersch, B. 1981. *Les hommes fossiles de Qafzeh (Israël)*. Éditions du C.N.R.S., Paris.
- Vandermeersch, B. 1991. La ceinture scapulaire et les membres supérieurs. In *Le Squelette Moustérien De Kébara 2*, Bar-Yosef, O. and Vandermeersch, B. (eds.). Éditions du CNRS, Paris, pp. 157–178.
- Villotte, S., Samsel, M., and Sparacello, V. 2017. The paleobiology of two adult skeletons from Baouso da Torre (Bausu da Ture) (Liguria, Italy): implications for Gravettian lifestyle. *Comptes Rendus Palevol* 16, 462–473.
- Watanabe, H. 1970. A Paleolithic industry from Amud Cave. In *The Amud Man and His Cave Site*, Suzuki, H. and Takai, F. (eds.). Academic Press of Japan, Tokyo, pp. 77–114.
- Wei, W., Ayub, Q., Chen, Y., McCarthy, S., Hou, Y., Carbone, I., Xue, Y., and Tyler-Smith, C. 2012. A calibrated human Y-chromosomal phylogeny based on resequencing. *Genome Research* 23, 388–395.

Weiner, S., Goldberg, P., and Bar-Yosef, O. 1993. Bone preservation in Kebara Cave, Israel using on-site Fourier Transform Infrared spectrometry. *Journal of Archaeological Science* 20, 613–627.

Zeigen, C., Shaar, R., Ebert, Y., and Hovers, E. 2019. Ar-

chaemagnetism of burnt cherts and hearths from Middle Palaeolithic Amud Cave, Israel: tools for reconstructing site formation processes and occupation history. *Journal of Archaeological Science* 107, 71–86.

## APPENDIX

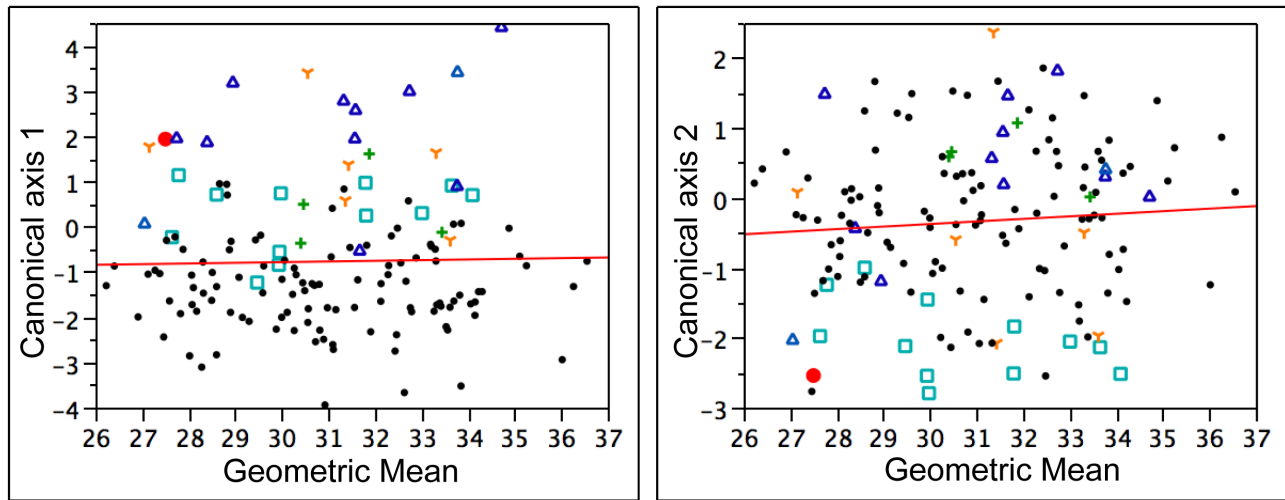


Figure A-1. Plots of canonical axis 1 and 2 from the CVA on raw data for the talus versus the geometric means of individuals in the analysis. In both cases, the geometric means of the tali are not significantly related to scores on the axis. For axis 1,  $R^2=0.0005$ ,  $p=0.7836$ ,  $n=145$ . For axis 2,  $R^2=0.0059$ ,  $p=0.3593$ ,  $n=145$ . These results refute the hypothesis that taxonomic attribution is a function of size in this data set. Symbols: large red dot, Amud 9; small black dot, recent human; dark blue triangle, Neandertal; teal square, Sima de los Huesos; green plus, Upper Paleolithic; orange Y, Middle Paleolithic modern human.

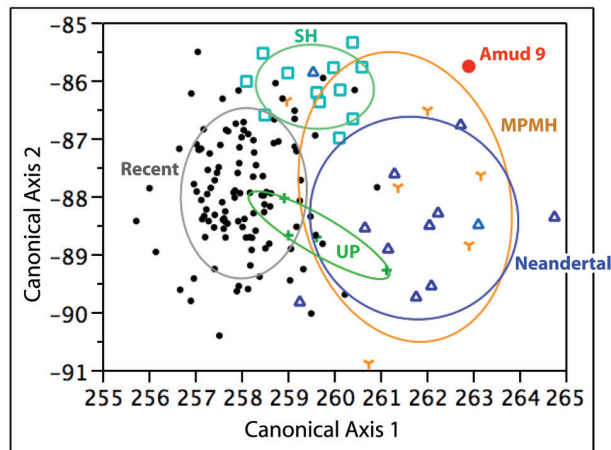


Figure A-2. Discriminant analysis of the talus (shape data). A 67% density ellipse surrounds each group's centroid. Abbreviations: MPMH, Middle Paleolithic modern humans; SH, Sima de los Huesos; UP, Upper Paleolithic.

**TABLE A-1. DETAILS OF THE DISCRIMINANT ANALYSIS OF THE TALUS**  
(shape data – adjusted by the geometric mean of the variables for each individual).

	Axis 1	Axis 2	Axis 3
<b>Eigenvalue:</b>	1.5570	0.3130	0.1547
<b>Percent variance:</b>	74.35	14.95	7.39
<b>Cumulative percent:</b>	74.35	89.30	96.69
	Eigenvector 1	Eigenvector 2	Eigenvector 3
<b>M1</b>	10.46	2.32	28.02
<b>M2</b>	31.45	-8.13	19.65
<b>M3</b>	32.45	-14.88	38.79
<b>M4</b>	20.86	-14.52	31.08
<b>M5</b>	22.43	-12.89	31.47
<b>M5-1</b>	35.55	-3.71	32.69
<b>M8</b>	26.64	-24.33	41.23
<b>M9</b>	26.50	-22.85	25.70
<b>M10</b>	31.57	-14.27	43.97
<b>M12</b>	25.62	-10.56	35.45

**TABLE A-2. POSTERIOR GROUP ASSIGNMENTS FROM THE CVA ON THE TALUS**  
(shape data – adjusted by the geometric mean of the variables for each individual).

Actual rows by assigned columns	MPMH	Neandertals	Recent	SH	UP
<b>MPMH</b>	4 (66.7%)	1 (16.7%)	0 (0%)	1 (16.7%)	0 (0%)
<b>Neandertals</b>	1 (5.9%)	12 (70.6%)	0 (0%)	2 (11.8%)	2 (11.8%)
<b>Recent</b>	3 (2.7%)	1 (0.9%)	84 (75.7%)	10 (9.0%)	13 (11.7%)
<b>SH</b>	0 (0%)	0 (0%)	0 (0%)	12 (100%)	0 (0%)
<b>UP</b>	0 (0%)	0 (0%)	2 (40%)	0 (0%)	3 (60%)
<b>Amud 9</b>	88.53%	10.03%	0%	1.44%	0%

The data in each cell show the number of tali assigned to the groups indicated in each column followed in parentheses by the percentage of individuals in the row. The values for Amud 9 show posterior probabilities of its assignment to each group. Abbreviations: MPMH, Middle Paleolithic Modern Humans; SH, Sima de los Huesos; UP, Upper Paleolithic.

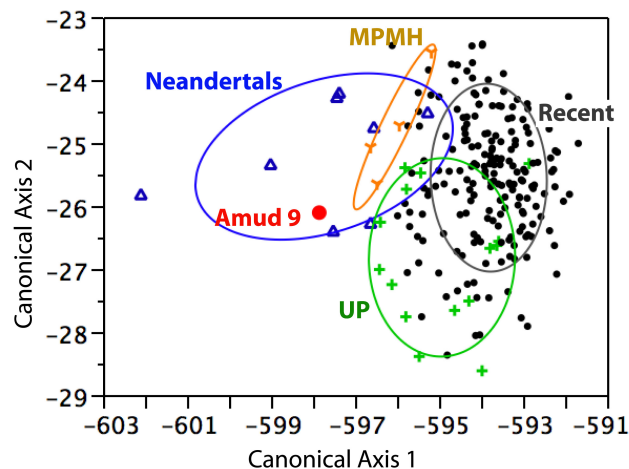


Figure A-3. Discriminant analysis of the first metatarsal (shape data). A 67% density ellipse surrounds each group's centroid. Abbreviations: MPMH, Middle Paleolithic modern humans; SH, Sima de los Huesos; UP, Upper Paleolithic.

**TABLE A-3. DETAILS OF THE DISCRIMINANT ANALYSIS OF THE METATARSAL**  
(shape data – adjusted by the geometric mean of the variables for each individual).

	Axis 1	Axis 2	Axis 3
<b>Eigenvalue:</b>	0.6760	0.1231	0.0489
<b>Percent variance:</b>	79.72	14.52	5.76
<b>Cumulative percent:</b>	79.72	94.24	100.0
	Eigenvector 1	Eigenvector 2	Eigenvector 3
<b>M1</b>	-26.75	-2.82	4.58
<b>M3</b>	-162.40	-4.98	35.23
<b>M4</b>	-126.13	-7.40	36.20
<b>M6</b>	-85.83	-1.38	7.43
<b>M7</b>	-73.94	5.63	2.18
<b>M8</b>	-89.18	4.03	15.42
<b>M9</b>	-98.01	-22.63	14.04

**TABLE A-4. POSTERIOR GROUP ASSIGNMENTS**  
**FROM THE CVA ON THE FIRST METATARSAL**  
(shape data – adjusted by the geometric mean of the variables for each individual).

Actual rows by assigned columns	MPMH	Neandertals	Recent	UP
<b>MPMH</b>	4 (100%)	0 (0%)	0 (0%)	0 (0%)
<b>Neandertals</b>	1 (10%)	9 (90%)	0 (0%)	0 (0%)
<b>Recent</b>	11 (5.7%)	2 (1.0%)	146 (75.3%)	35 (18.0%)
<b>UP</b>	0 (0%)	4 (17.4%)	7 (30.4%)	12 (52.2%)
<b>Amud 9</b>	8.35%	89.57%	0.05%	2.04%

The data in each cell show the number of tali assigned to the groups indicated in each column followed in parentheses by the percentage of individuals in the row. The values for Amud 9 show posterior probabilities of its assignment to each group. Abbreviations: MPMH, Middle Paleolithic Modern Humans; SH; UP, Upper Paleolithic.